iScience

CellPress

Article

High-Throughput Preparation of Antibacterial Polymers from Natural Product Derivatives via the Hantzsch Reaction

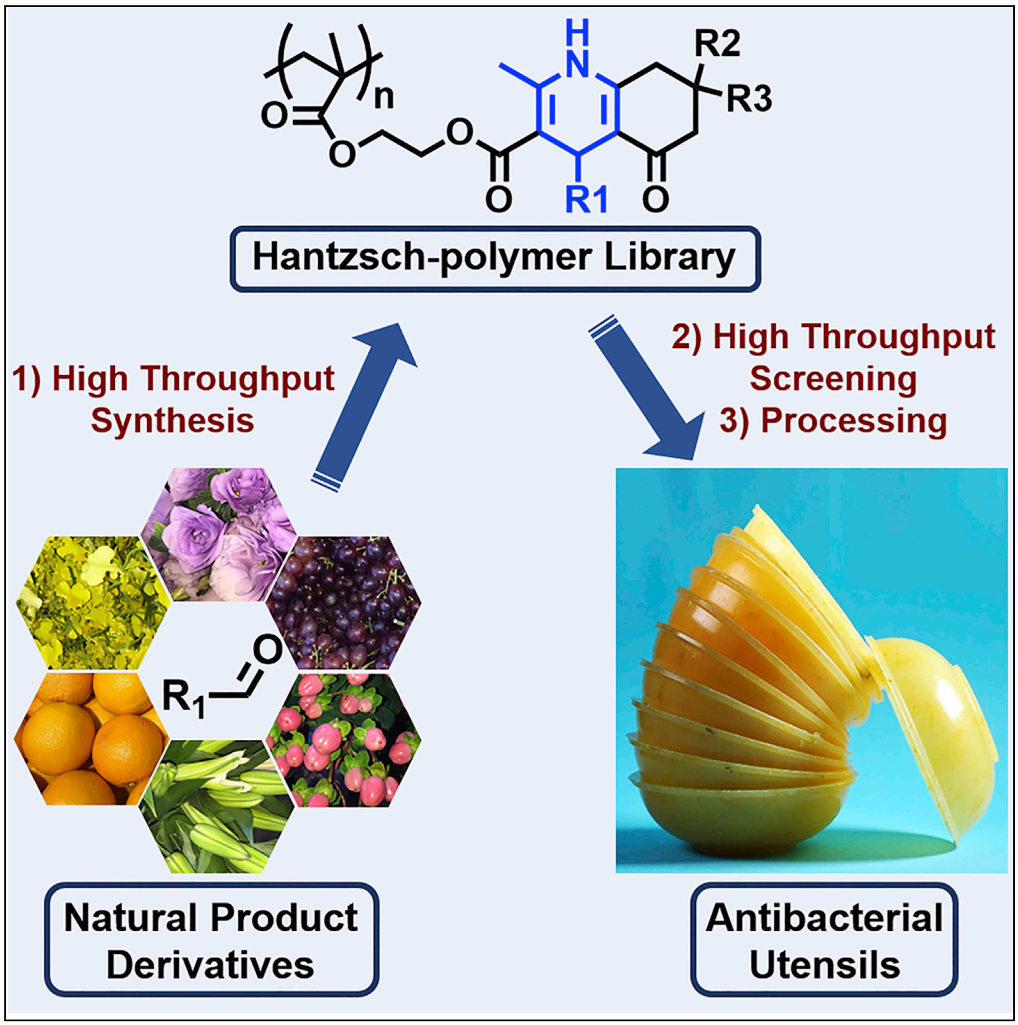

Guoqiang Liu, Qiang Zhang, Yongsan Li, ..., Yen Wei, Yuan Zeng, Lei Tao

leitao@mail.tsinghua.edu.cn

HIGHLIGHTS

A one-pot high-throughput (HTP) system was developed to prepare a polymer library

A new antibacterial polymer was selected from this library via HTP measurements

This antibacterial polymer was mixed in polyethylene to get antibacterial utensils

Mechanism study revealed that the Hantzsch reaction leads to new antibacterial polymers

Liu et al., iScience 23, 100754 January 24, 2020
https://doi.org/10.1016/j.isci.2019.100754

iScience

CellPress

Article

High-Throughput Preparation of Antibacterial Polymers from Natural Product Derivatives via the Hantzsch Reaction

Guoqiang Liu,[1] Qiang Zhang,[2] Yongsan Li,[1] Xing Wang,[3] Haibo Wu,[1] Yen Wei,[1] Yuan Zeng,[1] and Lei Tao[1,4,*]

SUMMARY

The Hantzsch and free-radical polymerization reactions were combined in a one-pot high-throughput (HTP) system to simultaneously prepare 30 unique polymers in parallel. Six aldehydes derived from natural products were used as the starting materials to rapidly prepare the library of 30 poly(1,4-dihydropyridines). From this library, HTP evaluation methods led to the identification of an antibacterial polymer. Mechanistic studies revealed that the dihydropyridine group in the polymer side-chain structure plays an important role in resisting bacterial attachment to the polymer surface, thus leading to the antibacterial function of this polymer. This research demonstrates the value of multicomponent reactions (MCRs) in interdisciplinary fields by discovering functional polymers for possible practical applications. It also provides insights to further developing new functional polymers using MCRs and HTP methods with important implications in organic chemistry, polymer chemistry, and materials science.

INTRODUCTION

High-throughput (HTP) synthesis methods enable the rapid production of hundreds to even millions of samples for screening and identifying products with the desired properties/functions (Briceno et al., 1995; Danielson et al., 1997; Hanak, 1970; Lehn and Eliseev, 2001; Rademann and Jung, 2000; Xiang et al., 1995). This effectively accelerates the pace of research, significantly increasing productivity and resulting in remarkable benefits. In polymer chemistry, HTP strategies have been successfully applied to the discovery of new functional polymers. Many polymers have been synthesized in parallel and characterized via HTP methods for detailed studies of the subtle relationships between polymer structures and properties. As a result, many new functional polymers have been explored and used in interdisciplinary fields as sensors, gene/drug carriers, antibacterial surfaces, tissue engineering scaffolds, (stem)cell factories, etc.(Akinc et al., 2003; Algahtani et al., 2014; Anderson et al., 2004, 2005, 2006; Bosman et al., 2001; Celiz et al., 2014; Chapman et al., 2016; Goldberg et al., 2008; Gupta et al., 2010; Hook et al., 2012; Khan et al., 2010; Lynn et al., 2001; Mao et al., 2018; Mei et al., 2010; Meier et al., 2004a, 2004b; Neumann et al., 2017; Ting et al., 2015, 2016). This has opened new research directions in polymer science and expanded the application scope of polymers beyond traditional plastics and rubbers. Thus, the development of new HTP methods to synthesize, screen, and isolate new polymers with application values is important from both academic and industrial points of view.

Multicomponent reactions (MCRs) are defined as reactions where three or more reactants combine to effectively generate a single product. Recently, MCRs have aroused widespread attention in polymer chemistry because Meier and coworkers reported the synthesis of polycondensates via the tricomponent Passerini reaction (Kreye et al., 2011). Since that report, more and more MCRs have been exploited for the preparation of elegant polymers containing multicomponent main chains and side chains. Such MCRs include the Passerini, Ugi, Mannich, Biginelli, Hantzsch, and Kabachnik-Fields reactions, as well as metal-catalyzed and thiolactone-based MCRs (Blasco et al., 2017; Deng et al., 2012; Espeel et al., 2011; Kakuchi and Theato, 2014; Kreye et al., 2011; Lee et al., 2013; Liu et al., 2014; Llevot et al., 2017; Sehlinger et al., 2013; Siamaki et al., 2011; Theato, 2015; Wu et al., 2017a; Zhang et al., 2014, 2016; Zhao et al., 2016).

MCRs have been applied to the construction of polymer libraries in an HTP manner (Mao et al., 2018; Wu et al., 2017b; Xue et al., 2016). MCRs quickly increase the number and diversity of polymer samples, owing to their multicomponent nature, effectively improving the synthesis efficiency for constructing polymer libraries. Selected robust MCRs have been carried out during controlled radical polymerization (CRP) to

[1]The Key Laboratory of Bioorganic Phosphorus Chemistry & Chemical Biology (Ministry of Education), Department of Chemistry, Tsinghua University, Beijing 100084, P. R. China

[2]Jiangsu Key Laboratory of Chemical Pollution Control and Resources Reuse, School of Environmental and Biological Engineering, Nanjing University of Science and Technology, Nanjing 210094, P. R. China

[3]Beijing Laboratory of Biomedical Materials, Beijing University of Chemical Technology, Beijing 100029, P. R. China

[4]Lead Contact

*Correspondence: leitao@mail.tsinghua.edu.cn

https://doi.org/10.1016/j.isci.2019.100754

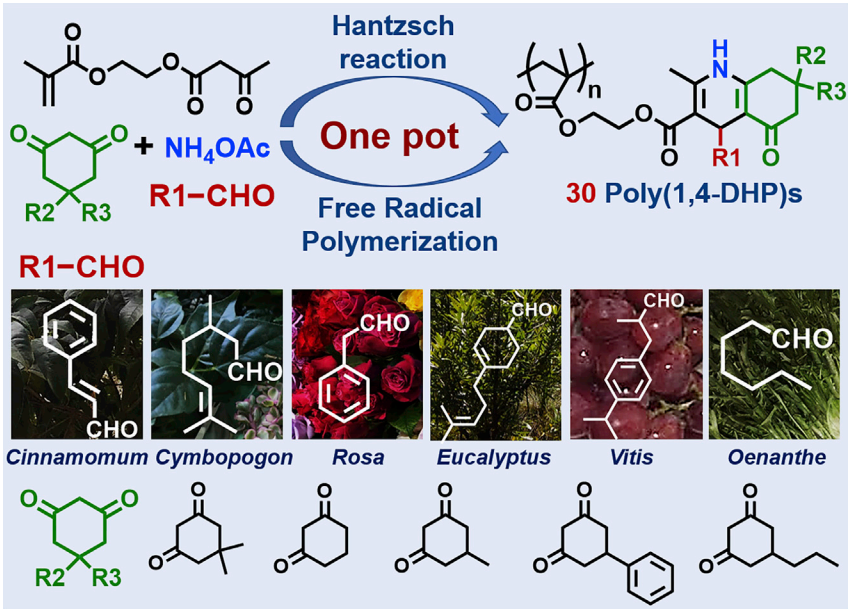

Scheme 1. One-Pot HTP Method for Preparing a Library of Poly(1,4-DHP)s

successfully prepare well-defined polymers with multicomponent pendant/chain end groups in a one-pot manner (Yang et al., 2015; Zhang et al., 2014, 2015; Zhu et al., 2013). This greatly simplifies the preparation of new polymers by avoiding the tedious separation and purification steps during a new monomer/initiator synthesis. HTP methods, MCRs, and a one-pot strategy straightforwardly improve the efficiency of polymer preparation; thus, the combination of HTP methods, MCRs, and a one-pot strategy might lead to a new methodology for facilely constructing polymer libraries. Herein, we report a one-pot HTP method that can quickly establish a library of poly(1,4-dihydropyridine)s (poly(1,4-DHP)s) via the Hantzsch reaction (a typical MCR) and free-radical polymerization (FRP) (Scheme 1).

The Hantzsch reaction, reported by Arthur R. Hantzsch in 1881(Hantzsch, 1881), consists of four common components (aldehyde, β-ketoester, 1,3-diketone, and NH_4OAc) and effectively produces 1,4-dihydropyridines (1,4-DHPs), which are candidate drugs for treating cardiovascular diseases (Loev et al., 1974; Stout and Meyers, 1982). The Hantzsch reaction has been broadly studied in organic chemistry and pharmaceutical chemistry; only recently has this venerable reaction been explored in polymer chemistry. Well-defined polymers with 1,4-DHP side groups have been efficiently prepared by the combination of the Hantzsch reaction and reversible addition-fragmentation chain transfer (RAFT) polymerization in a one-pot fashion (Zhang et al., 2015). Here, we chose FRP instead of CRP to further simplify the polymerization process. Aldehydes derived from natural products were reacted with a commercially available monomer, 2-(acetoacetoxy) ethyl methacrylate (AEMA), via the Hantzsch reaction during the FRP process. The polymers were synthesized in parallel using one-pot reactions containing different combinations of six aldehydes (**A(X)**) and five 1,3-cyclohexanedione compounds (**B(Y)**) to simultaneously create 6 × 5 = 30 unique polymers (P(X) (Y)).

The resulting polymers were fully characterized by NMR, gel permeation chromatography (GPC), thermal gravimetric analysis (TGA), and differential scanning calorimetry (DSC) to determine the polymerization conversions and investigate polymer properties. These polymers were then screened via HTP measurement techniques to ultimately identify the polymer with the best antibacterial ability. This polymer was then blended with commodity polymers (polyethylene [PE], poly(propene) [PP], poly(ethylene terephthalate) [PET], poly(methyl methacrylate) [PMMA], and polyamide [PA66]) to dramatically improve the antibacterial ability of these general polymers without impairing the mechanical strength of the overall polymer system. This research used the Hantzsch reaction and HTP methods to develop antibacterial polymers via a green chemistry approach by utilizing aldehydes derived from natural sources instead of oil-based products. This demonstrates the utility of synthesis strategies in polymer chemistry to explore functional polymers for practical applications.

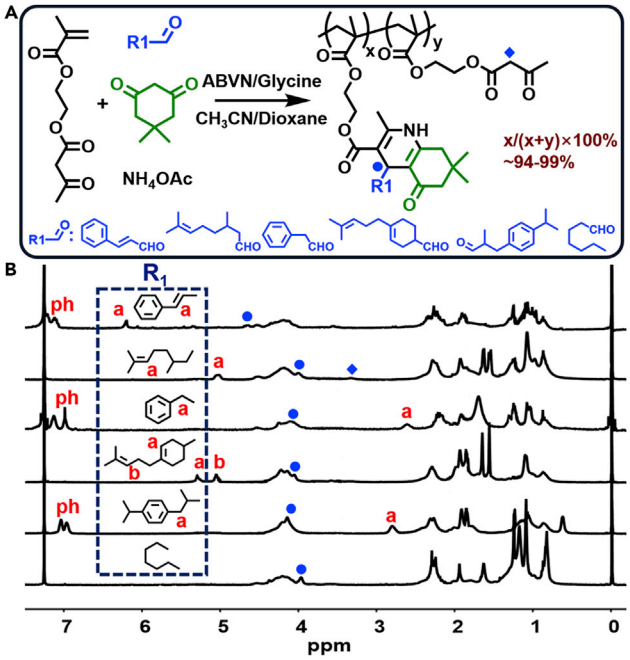

Figure 1. Preparation of P(X)(1)

(A) Reaction conditions: acetonitrile/dioxane (1/1, v/v), glycine (10% to aldehydes), ABVN (2% to AEMA), 75°C for 12 h. A(X): B(1): AEMA: NH_4OAc = 1:1:1:1.5.

(B) ^1H NMR spectra ($CDCl_3$, 400M) of P(X) (1).

RESULTS AND DISCUSSION

One-Pot HTP Preparation of Polymers via the Hantzsch Reaction and FRP

In a representative procedure, **A(X)**, **B(Y)**, AEMA, and NH_4OAc were added to centrifuge tubes; the molar ratio of each component was **A(X)**: **B(Y)**: AEMA: NH_4OAc = 1:1:1:1.5. Solvents (acetonitrile and 1,4-dioxane [1/1, v/v]) were then added followed by glycine (10 mol% with respect to aldehydes) and 2,2′-azobisisoheptonitrile (ABVN, 2 mol% to AEMA) as the catalyst for the Hantzsch reaction and the FRP initiator, respectively. The 30 charged tubes were purged with bubbling nitrogen for 20 min and then immersed in a 75°C oil bath for 12 h. After quenching the polymerization in an ice-water bath, aliquots (20–50 μL) were taken for ^1H NMR and GPC analyses. For every tube, AEMA was polymerized in high conversions (95%–99%), and the peaks associated with β-ketoester groups of AEMA nearly completely disappeared (92%–99%) (Figure S1 [**P(X) (1)** as a typical example], Table S1). All poly(1,4-DHP)s had high molecular weights (M_n(GPC): 16,000–28,000 g mol^{-1}, Figure S2 [**P(X) (1)** as a typical example], Table S1). It is noticed that P(5) (Y) have broader polydispersity indices (PDIs) than others. This might be attributed to the iso-propylbenzene moieties in P(5) (Y). The iso-propylbenzene group is capable of producing radical during polymerization (Gregg and Mayo, 1947; Okamura and Katagiri, 1958). The iso-propylbenzene radical in polymer structures might link other polymer chains leading to broad PDIs.

The **P(X) (Y)** were purified through simple precipitation in water followed by re-precipitation from tetrahydrofuran by diethyl ether. As a typical example, the ^1H NMR spectra of P(X) (1) are presented in Figure 1.

The specific peaks of the 1,4-DHP moieties (R1-CH) can be found at 3.95–4.55 ppm, whereas the peaks of the AEMA vinyl group (6.07, 5.55 ppm) have completely disappeared. The unreacted β-ketoesters (~3.48 ppm) in P(X) (1) were calculated as ~1%–6% (Table S1). Other P(X) (Y) polymers showed similar results (Figures S3–S6, Table S1). Thus, the selected aldehydes and 1,3-cyclohexanedione derivatives were suitable components for the Hantzsch reaction and highly compatible with FRP.

To compare the effectiveness of the one-pot HTP method with the traditional monomer polymerization approach, **P(X) (1)** with 100% 1,4-DHP side groups were prepared in a two-step process (Figures S7–S12). As a typical example, cinnamaldehyde (**A(1)**) was reacted with AEMA and dimedone (**B(1)**) via the

Hantzsch reaction to obtain the target monomer **M(1) (1)** in 73.6% yield after column chromatography purification. **M(1) (1)** was polymerized through FRP to obtain the desired "pure" polymer **P(1) (1)**. ^{1}H NMR spectra indicated that this polymer was nearly identical to that obtained by the one-pot HTP method (Figure S7). Similar results were observed when other aldehydes were used to prepare pure monomers and polymers (Figures S8–S12). This suggests the feasibility of this one-pot HTP strategy to quickly build a library of target polymers in a time-saving and labor-saving manner.

HTP Analyses of the Antibacterial Capabilities of P(X) (Y)

1,4-DHP derivatives have been reported as potential antimicrobial agents, antioxidants, and anti-inflammatory agents (Vijesh et al., 2011). The selected aldehydes in this study have been widely employed in the cosmetic, food, and pharmaceutical industries as flavor agents, antibacterial agents, and antioxidants (Aziz and Karboune, 2018; Gyawali and Ibrahim, 2014). Thus, this library of poly(1,4-DHP)s might contain new functional polymers with bioactive properties. To test this hypothesis, the antibacterial capability of the resulting polymers was evaluated via HTP measurement techniques.

Preliminary Screening

The resulting polymers were mixed with poly(ethylene) (PE) to prepare mixed hot-pressed samples. The weight ratio of P(X) (Y) in P(X) (Y)-PE was 33%, and the actual polymer concentrations on PE surface were found to range from 27.0% to 39.9% by X-ray photoelectron spectroscopy (XPS) analyses (Table S2). *Escherichia coli* and *Staphylococcus aureus* were used as representative Gram-negative and Gram-positive bacteria, respectively. Both bacteria were transfected with red fluorescent protein (RFP) for easy observation.

Briefly, 30 disk samples of P(X) (Y)-PE (diameter: 5 mm, thickness: 0.5 mm) were attached to three pieces of glass to form three mini-arrays (Figure 2A, 10 samples/piece). Pure PE disks served as the control. These polymer arrays were sterilized by a 75% ethanol aqueous solution and UV light irradiation (254 nm, 40 w, 30 min), then put into a Luria-Bertani (LB) broth (200 mL) followed by the addition of a suspension of planktonic *E. coli* or *S. aureus* (10 μL). The optical density of this suspension at UV ~ 600 nm (OD600) was approximately 1.0. The polymer arrays were incubated with bacteria for 72 h before observation by laser scanning confocal microscopy (LSCM) (Figure 2A). The fluorescence intensity at each sample disk reflected the number of attached bacteria.

From the LSCM images (Figures 2B and 2C), the P(X) (Y)-PE samples contained far fewer bacteria than the pure PE sample. This was interpreted as the antibacterial capability of these 1,4-DHP-containing polymers. The quantitative fluorescence intensity maps of the samples indicated almost no *E. coli* on **P(4) (1)**, **P(4) (3)**, **P(4) (4)**, and **P(5) (5)** (Figure 2B') and almost no *S. aureus* on **P(1) (4)**, **P(4) (1)**, **P(4) (3)**, **P(4) (4)**, and **P(4) (5)** (Figure 2C'). Meanwhile, mature biofilm might begin to disperse (Morimatsu et al., 2012; Steinberger et al., 2002); thus, these polymer samples have been tested with shorter culture time and/or lower nutrient medium (Figure S13: normal medium/24 h culture; Figure S14: 20% nutrient medium/72 h culture; Figure S15: 20% nutrient medium/24 h culture). More samples demonstrated excellent antibacterial capability to *E. coli* and *S. aureus* suggesting negligible biofilm generated during the mini-array experiment. Then, the antibacterial efficiency of all poly(1,4-DHP)s was calculated by comparing the fluorescence intensity on P(X) (Y)-PE and PE (Table S3, normal medium/72 h). **P(4) (1)**, **P(4) (3)**, and **P(4) (4)** demonstrated better antibacterial efficiency to both *E. coli* and *S. aureus* (>95%) than the other poly(1,4-DHP)s; thus, these three polymers were selected as the top three broad-spectrum antibacterial polymers for the next round of screening.

Secondary Screening

Commodity polymers are indispensable to everyday life. If items composed from these polymers can be imbued with antibacterial properties, the value of the items produced with such polymers would be increased greatly. Thus, the three best polymers from preliminary testing (Figure 3A) were blended into five commonly found commodity polymers (PE, PP, PET, PMMA, and PA66) in different ratios (33%, 20%, 10%, and 5%).

The antibacterial capabilities of these **P(4) (1,3,4)**-polymer samples were subjected to a similar test as before. Pure commodity polymer disks were used as the respective controls.

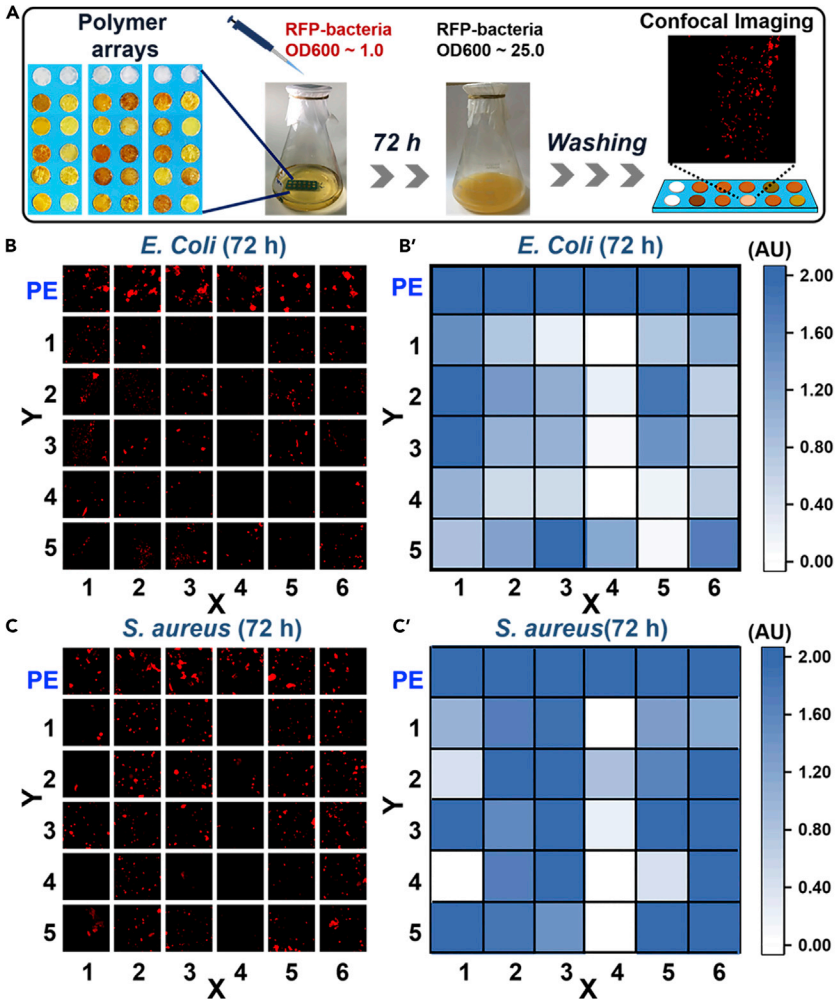

Figure 2. HTP analysis of the antibacterial capabilities of P(X) (Y)

(A) Schematic of the polymer arrays and the test procedure.

(B) LSCM images and (B′) intensity map of *E. coli* on sample disks after 72-h incubation. PE served as the control; each image is 200 × 200 μm. Three replicate samples were tested.

(C) LSCM images and (C′) intensity map of *S. aureus* on sample disks after 72-h incubation. PE served as the control; each image is 200 × 200 μm. Three replicate samples were tested.

The fluorescence intensity maps (Figures 3B and 3C; Table S4) were obtained according to the LSCM images (Figure S16). The greater the **P(4) (1,3,4)** content, the fewer the bacteria found on the **P(4) (1,3,4)**-polymer blends, indicative of a concentration-dependent antibacterial property. When the poly(1,4-DHP) to commodity polymer blend was 10 wt.%, **P(4) (4)** offered the best antibacterial properties. Thus, **P(4) (4)** was selected for further research.

Development of a Model Antibacterial Utensil

For items made from these commodity polymer-antibacterial polymer blends to remain practical, the basic mechanical properties of the base commodity polymer must not be meaningfully compromised. Thus, the mechanical strength of the **P(4) (4)**-polymer samples (33 wt.% **P(4) (4)**) was tested using PE, PP, PET, PMMA, and PA66 (Figure S17). All five 33 wt.% **P(4) (4)**-polymer samples yielded the similar mechanical strength results as the pure-polymer controls. This suggests that commodity polymers can be easily blended with antibacterial **P(4) (4)** without a loss of mechanical strength.

Next, we applied the injection molding technique to form antibacterial plastic products from a blended P(4) (4) and PE mixture. PE was chosen as a representative sample owing to its easy machining and broad

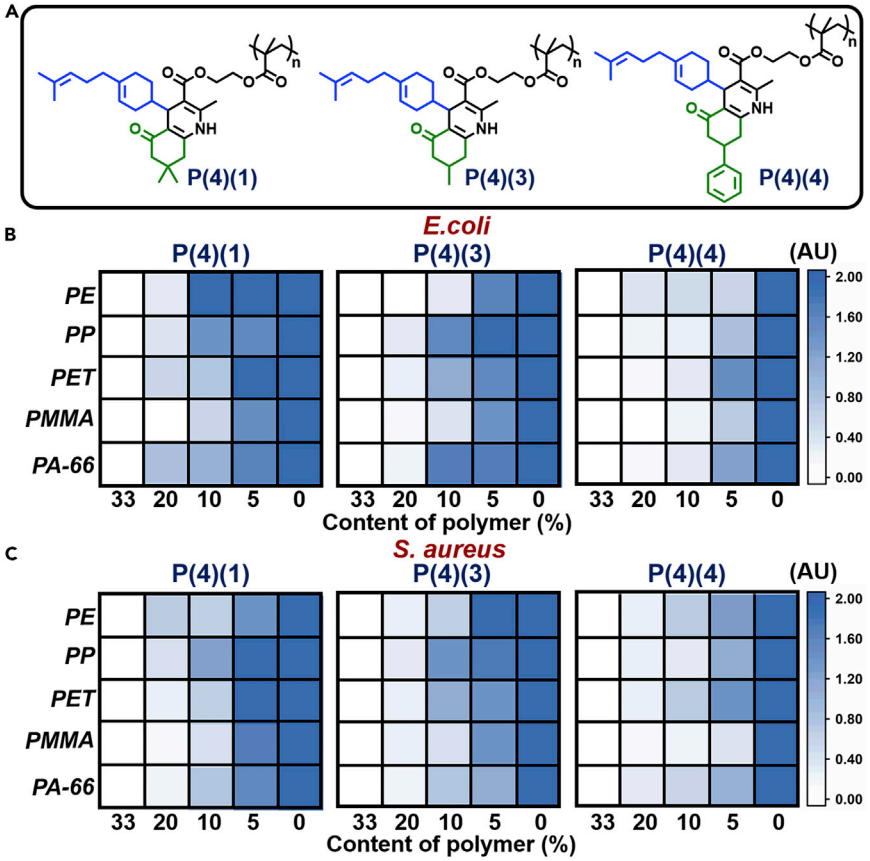

Figure 3. HTP analysis of the antibacterial capabilities of selected polymers

(A) The three poly(1,4-DHP)s selected for further study after preliminary tests.

(B and C) Intensity map of the bacteria on sample disks (commodity polymers + P(X) (Y)), 72 h culture. Three replicate samples were tested, and pure commodity polymer disks served as the controls.

applicability as a packaging material. P(4) (4)-PE (33 wt.% of P(4) (4)) and PE were injection molded into plastic bowls (Figure 4A, diameter: 44 mm, height: 14 mm).

An experiment was designed to evaluate the antibacterial ability of these bowls by simulating the actual application. Briefly, these bowls were sterilized by a 75% ethanol aqueous solution and air dried on a laboratory bench for 24 h. Then, various commonly consumed beverages (water, orange juice, milk, red wine, coffee, and black tea) (5 mL) were placed in the PE and P(4) (4)-PE bowls (Figure 4B). Glass covers were placed on the bowls, and the beverages were incubated at 37°C. Aliquots were obtained at specified time points.

A plate-streaking experiment was performed to test for the presence of viable bacteria. After 24 h, beverage aliquots (100 μL) from the different bowls were taken and evenly coated on the surface of LB agar-coated petri dishes (diameter: 90 mm, thickness: 6 mm, LB: 1.5 g/L). These petri dishes were incubated at 37°C before observation, and the original beverages were used as the controls (Figure 4C).

Commercially available beverages are typically sterile; thus, almost no bacterial colonies were observed (Figure 4C, control). However, aliquots of water, orange juice, milk, and coffee from the pure PE bowls clearly contained bacteria, as demonstrated by the visible colonies grown on the LB agar petri dishes (Figure 4C, PE). This suggests that the PE bowls were contaminated with germs when stored in the open air, leading to the contamination of these beverages inside. Notably, red wine and black tea samples from the pure PE bowls yielded similar results to the control during the LB agar growth test. This was attributed to the antibacterial compounds contained in the parent beverages, such as tannin, ethanol, and tea

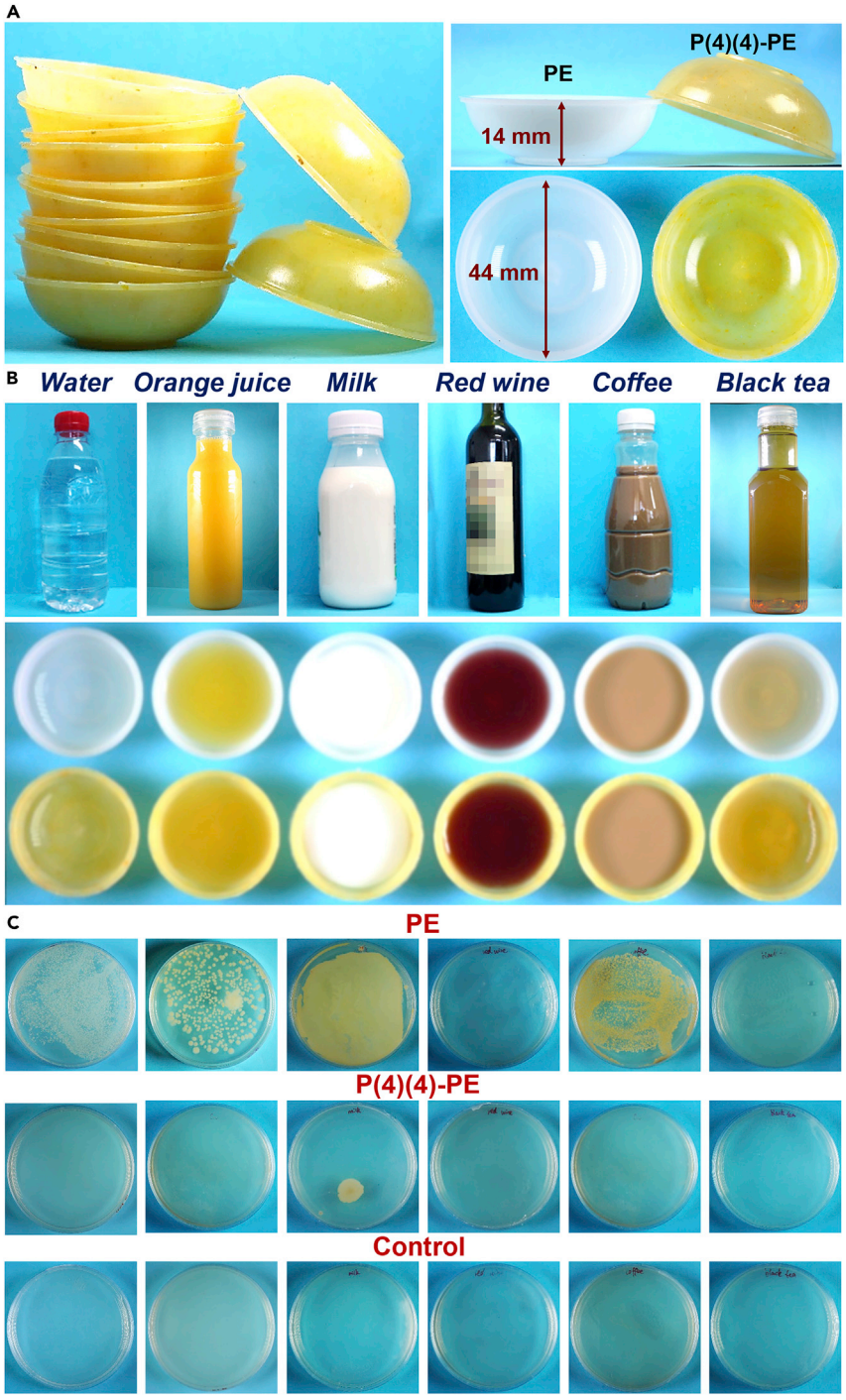

Figure 4. Antibacterial bowls made from P(4)(4)-PE

(A) Bowls made from PE and **P(4) (4)**-PE.

(B) Commercially available beverages (5 mL) for testing and the experimental setup.

(C) Photographic images of the plate-streaking experiment: 100 μL sample on LB agar (15 g/L), 24-h culture.

polyphenols (Figure 4C, PE). On the other hand, only milk in the **P(4) (4)**-PE bowl resulted in a small bacterial colony on the LB agar surface (Figure 4C, **P(4) (4)**-PE). This suggests that only milk contained sufficient nutrients to encourage growth of the small amount of bacteria present after 24 h of open-air storage and overcome the inherent antibacterial properties of the **P(4) (4)**-PE bowls.

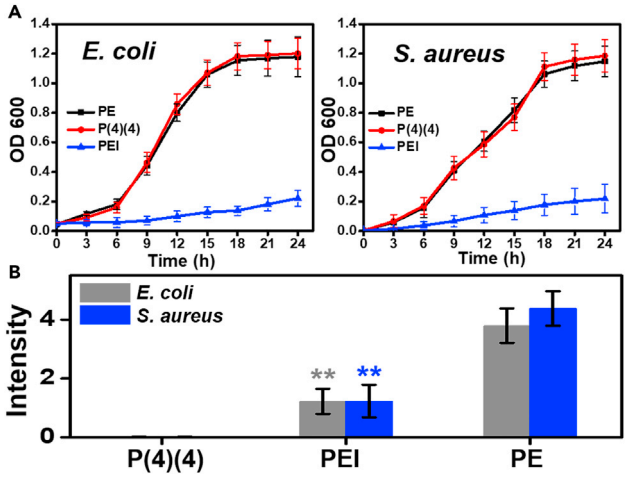

Figure 5. Evaluation of bactericidal ability of P(4)(4)-PE

(A) OD600 values versus time in the presence of different polymers, 24-h culture. Data are represented as mean ± SD, n = 5.

(B) Intensity data of bacteria on sample disks after 72-h incubation. Data are represented as mean ± SD, n = 3; **p < 0.01, compared with PE.

Additional samples were obtained after 48 and 72 h to repeat the plate-streaking experiments (Figure S18). Denser and denser bacterial colonies were observed in the pure PE group over time, indicating propagation of bacteria in beverages incubated in the pure PE bowls. The inherent antibacterial defenses of tea and red wine expired after 48 and 72 h, respectively. Nevertheless, all beverages, except milk, in the **P(4) (4)**-PE bowls remained bacteria-free after 48 h of incubation (Figure S18A). Red wine and tea in **P(4) (4)**-PE bowls remained sterile even after 72-h incubation (Figure S18B). These results agreed well with the quantitative OD600 analyses (Figure S19).

Furthermore, a quantitative experiment was performed according to a standard method (QB/T2591-2003) to evaluate the antibacterial capability of these bowls. The bowls were incubated with *S. aureus* (an approved model bacterium, 5 mL, LB medium, OD600 ~1.0) for 24 h at 37°C, then washed by sterilized PBS followed by addition of beverages (5 mL). A plate-streaking experiment and OD600 analyses were performed at different time points to test viable bacteria (Figures S20 and S21). The antibacterial results obtained by this way are similar to those obtained by the previous method, suggesting great potential for the **P(4) (4)**-PE blended polymer as a new antibacterial material for utensils and food applications.

Mechanism Study

The possible mechanisms for antibacterial action of **P(4) (4)** were studied. Several polymers were used according to the different evaluation protocols.

Bactericidal Ability

Killing bacteria is a general strategy in developing antibacterial materials. Some 1,4-DHPs have been reported to effectively inhibit bacterial growth. Thus, the bactericidal ability of **P(4) (4)** was evaluated. Polyetherimide (PEI), a well-known antibacterial polymer that is lethal to bacteria(Gibney et al., 2012), was used as the control. **P(4) (4)**-PE (33 wt.% **P(4) (4)**) and PEI-PE (33 wt.% PEI) disks were prepared as mentioned earlier. These two samples were attached to the bottom of a multi-well plate and covered with LB broth (200 μL). Then, a suspension of planktonic *E. coli* or *S. aureus* (10 μL, OD600~1.0) was added. The plate was incubated at 37°C for 24 h. The OD600 values were tested at different time intervals, and a pure PE disk was used as the blank control.

From the OD600 curves over time (Figure 5A), the rate of bacterial growth was slower with PEI-PE than with **P(4) (4)**-PE and PE, confirming the ability of PEI to kill bacteria. There was no observable difference in bacterial growth rates between **P(4) (4)**-PE and PE. This suggests that **P(4) (4)** has negligible bactericidal effects. Thus, P(4) (4) likely achieves its antibacterial function by preventing bacterial adhesion or biofilm

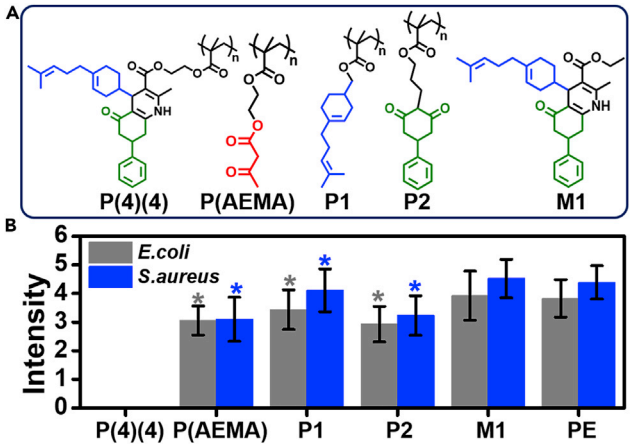

Figure 6. Relationship between the structure of P(4)(4) and its antibacterial ability

(A) P(4) (4), P(AEMA), P1 (polymer containing a long-branched olefin), P2 (polymer containing an aromatic group), and M1.

(B) Intensity data of bacteria on sample disks after a 72-h culture. Data are represented as mean ± SD, n = 3; *p < 0.05, compared with PE.

formation instead of killing the bacteria outright. Moreover, **P(4) (4)** has weaker interaction than PE with lipopolysaccharide and peptidoglycan, two polysaccharides on the bacterial surface (Table S5). This suggests that the interaction of P(4) (4) with the cell membrane may play a role in its ability to prevent biofilm formation.

Then, the antibacterial abilities of samples were evaluated through the polymer-array method. After 72-h incubation, PEI effectively killed bacteria, resulting in much less bacteria on the PEI-PE surface than on PE (Figure 5B, $p < 0.01$ compared with PE; Figure S22). However, almost no bacteria was detected on the **P(4) (4)**-PE surface despite the poor sterilization ability of **P(4) (4)** (Figures 5B and S22).

Molecular Structures

Polymer functions are determined by their molecular structures. Thus, the relationship between the structure of **P(4) (4)** and its antibacterial ability was studied.

The Hantzsch ring in **P(4) (4)** is composed of a long-branched olefin and aromatic groups. There are still some β-ketoester moieties (~2%) left in **P(4) (4)**. Thus, two polymers containing only the long-branched olefin and aromatic groups were prepared (Figures 6A, **P1**, **P2**; S23, and S24). A homopolymer of AEMA was also prepared (Figures 6A, P(AEMA) and S25). Meanwhile, a small molecule with similar Hantzsch ring as the side group of **P(4) (4)** was prepared (Figure 6A, **M1**). These polymers (**P1**, **P2**, P(AEMA)) and **M1** were mixed with PE to prepare samples, respectively. The antibacterial capabilities of these samples were studied via the polymer-array method. The sample composed of pure PE served as the blank.

The fluorescence signals of *E. coli* and *S. aureus* on the polymer samples were recorded (Figure S26). Quantitative data from the fluorescence intensity were calculated, and the number of bacteria present on the samples followed the order **P(4) (4)** << P(AEMA) ≈ **P2** < **P1** < M1 ≈ PE (Figure 6B). M1 concentration on the PE surface was tested by XPS as 29.5% (Table S2), and M1-PE had almost no antibacterial ability ($p = 0.118$ [*E. coli*], 0.137 [*S. aureus*], compared with PE), suggesting that direct addition of free 1,4-DHP molecules to bulk commodity polymers would not be effective. **P1**, **P2**, and P(AEMA) demonstrated poor antibacterial capability ($p < 0.05$, compared with PE), whereas **P(4) (4)** had the best antibacterial ability among all poly(1,4-DHP)s. These results suggest the polymer chain and 1,4-DHP pendant group both play key roles for the antibacterial function of **P(4) (4)**; the long-branched olefin and aromatic groups enhance the antibacterial ability of **P(4) (4)** via a possible synergistic effect.

Limitation of the Study

Here, a simple polymer (random structure with a broad PDI) with potential antibacterial applications was developed via a very simple HTP method (small sample pool and semiquantitative measurements). This

highlights the validity of HTP methods and MCRs in exploring new functional polymers. However, in addition to side-chain groups, the core polymer structure can also be important for polymer functions. Recent studies have reported that the antibacterial capability of polymers can be remarkably improved by tuning the polymer structures (i.e., monomer sequences and topology structures) (Judzewitsch et al., 2018; Kuroki et al., 2017; Lam et al., 2016; Namivandi-Zangeneh et al., 2018). Currently, well-defined polymers can be rapidly prepared via modern technologies in CRP, including single electron transfer-atom transfer radical polymerization (SET-ATRP), sulfur-free RAFT emulsion polymerization, photoinduced ATRP, and photoinduced electron/energy transfer-RAFT (PET-RAFT) (Anastasaki et al., 2014, 2016; Boyer et al., 2016; Carmean et al., 2017; Chen et al., 2016; Engelis et al., 2017; Fors and Hawker, 2012; Gormley et al., 2018; Rosen and Percec, 2009; Xu et al., 2016; Zhang et al., 2013). The future combination of these modern CRP techniques with the method used here might offer new polymer libraries with different side groups, molecular weights, monomer sequences, topology structures, etc. This will be helpful for developing new polymers with improved antibacterial capabilities and other bioactive functions.

Conclusions

In summary, we have developed a one-pot HTP method by simultaneously carrying out the Hantzsch reaction and FRP in an HTP manner. Using this method, six aldehydes derived from natural products were used to rapidly synthesize 30 poly(1,4-DHP)s in one step. This highlighted the advantage of MCRs in amplifying molecular diversity and the superiority of a one-pot strategy in improving synthesis efficiency. The resulting poly(1,4-DHP)s were screened via HTP measurement methods to ultimately identify a polymer that could effectively resist bacterial attachment due to its unique 1,4-DHP side group. This opens the door to opportunities for developing antibacterial compounds via the Hantzsch reaction. The developed one-pot method highlighted the value of HTP methods, natural product derivatives, and MCRs for exploring new functional polymers with potential applications in the real world. These results might prompt a broad study of MCRs and HTP methods in polymer science for developing other new functional polymers for interdisciplinary applications.

METHODS

All methods can be found in the accompanying Transparent Methods supplemental file.

SUPPLEMENTAL INFORMATION

Supplemental Information can be found online at https://doi.org/10.1016/j.isci.2019.100754.

ACKNOWLEDGMENT

This research was supported by the National Science Foundation of China (21574073, 21971141).

AUTHOR CONTRIBUTIONS

L.T. developed the concept and conceived the experiments. G.L., Y.L., H.W., and Y.Z. performed the laboratory experiments. L.T., G.L., Q.Z., and X.W. contributed to the experimental analyses. L.T. and G.L. wrote the manuscript. L.T. and Y.W. provided financial support to the research.

DECLARATION OF INTERESTS

The authors declare no competing financial interests.

Received: July 19, 2019
Revised: November 25, 2019
Accepted: November 27, 2019
Published: January 24, 2020

REFERENCES

Akinc, A., Lynn, D.M., Anderson, D.G., and Langer, R. (2003). Parallel synthesis and biophysical characterization of a degradable polymer library for gene delivery. J. Am. Chem. Soc. *125*, 5316–5323.

Algahtani, M.S., Scurr, D.J., Hook, A.L., Anderson, D.G., Langer, R.S., Burley, J.C., Alexander, M.R., and Davies, M.C. (2014). High throughput screening for biomaterials discovery. J. Control Release *190*, 115–126.

Anastasaki, A., Nikolaou, V., Nurumbetov, G., Wilson, P., Kempe, K., Quinn, J.F., Davis, T.P., Whittaker, M.R., and Haddleton, D.M. (2016). Cu(0)-Mediated living radical polymerization: a versatile tool for materials synthesis. Chem. Rev. *116*, 835–877.

Anastasaki, A., Nikolaou, V., Zhang, Q., Burns, J., Samanta, S.R., Waldron, C., Haddleton, A.J., McHale, R., Fox, D., Percec, V., et al. (2014). Copper(II)/Tertiary amine synergy in photoinduced living radical polymerization: accelerated synthesis of omega-functional and alpha,omega-heterofunctional poly(acrylates). J. Am. Chem. Soc. *136*, 1141–1149.

Anderson, D.G., Peng, W.D., Akinc, A., Hossain, N., Kohn, A., Padera, R., Langer, R., and Sawicki, J.A. (2004). A polymer library approach to suicide gene therapy for cancer. Proc. Natl. Acad. Sci. U S A *101*, 16028–16033.

Anderson, D.G., Putnam, D., Lavik, E.B., Mahmood, T.A., and Langer, R. (2005). Biomaterial microarrays: rapid, microscale screening of polymer-cell interaction. Biomaterials *26*, 4892–4897.

Anderson, D.G., Tweedie, C.A., Hossain, N., Navarro, S.M., Brey, D.M., Van Vliet, K.J., Langer, R., and Burdick, J.A. (2006). A combinatorial library of photocrosslinkable and degradable materials. Adv. Mater. *18*, 2614–2618.

Aziz, M., and Karboune, S. (2018). Natural antimicrobial/antioxidant agents in meat and poultry products as well as fruits and vegetables: a review. Crit. Rev. Food Sci. *58*, 486–511.

Blasco, E., Sims, M.B., Goldmann, A.S., Sumerlin, B.S., and Barner-Kowollik, C. (2017). 50th anniversary perspective: polymer functionalization. Macromolecules *50*, 5215–5252.

Bosman, A.W., Heumann, A., Klaerner, G., Benoit, D., Frechet, J.M.J., and Hawker, C.J. (2001). High-throughput synthesis of nanoscale materials: structural optimization of functionalized one-step star polymers. J. Am. Chem. Soc. *123*, 6461–6462.

Boyer, C., Corrigan, N.A., Jung, K., Nguyen, D., Nguyen, T.K., Adnan, N.N.M., Oliver, S., Shanmugam, S., and Yeow, J. (2016). Copper-mediated living radical polymerization (atom transfer radical polymerization and copper(0) mediated polymerization): from fundamentals to bioapplications. Chem. Rev. *116*, 1803–1949.

Briceno, G., Chang, H.Y., Sun, X.D., Schultz, P.G., and Xiang, X.D. (1995). A class of cobalt oxide magnetoresistance materials discovered with combinatorial synthesis. Science *270*, 273–275.

Carmean, R.N., Becker, T.E., Sims, M.B., and Sumerlin, B.S. (2017). Ultra-high molecular weights via aqueous reversible-deactivation radical polymerization. Chem *2*, 93–101.

Celiz, A.D., Smith, J.G.W., Langer, R., Anderson, D.G., Winkler, D.A., Barrett, D.A., Davies, M.C., Young, L.E., Denning, C., and Alexander, M.R. (2014). Materials for stem cell factories of the future. Nat. Mater. *13*, 570–579.

Chapman, R., Gormley, A.J., Stenzel, M.H., and Stevens, M.M. (2016). Combinatorial low-volume synthesis of well-defined polymers by enzyme degassing. Angew. Chem. Int. Ed. *55*, 4500–4503.

Chen, M., Zhong, M.J., and Johnson, J.A. (2016). Light-controlled radical polymerization: mechanisms, methods, and applications. Chem. Rev. *116*, 10167–10211.

Danielson, E., Golden, J.H., McFarland, E.W., Reaves, C.M., Weinberg, W.H., and Wu, X.D. (1997). A combinatorial approach to the discovery and optimization of luminescent materials. Nature *389*, 944–948.

Deng, X.X., Li, L., Li, Z.L., Lv, A., Du, F.S., and Li, Z.C. (2012). Sequence regulated poly(ester-amide)s based on Passerini reaction. ACS Macro. Lett. *1*, 1300–1303.

Engelis, N.G., Anastasaki, A., Nurumbetov, G., Truong, N.P., Nikolaou, V., Shegiwal, A., Whittaker, M.R., Davis, T.P., and Haddleton, D.M. (2017). Sequence-controlled methacrylic multiblock copolymers via sulfur-free RAFT emulsion polymerization. Nat. Chem. *9*, 171–178.

Espeel, P., Goethals, F., and Du Prez, F.E. (2011). One-pot multistep reactions based on thiolactones: extending the realm of thiol-ene chemistry in polymer synthesis. J. Am. Chem. Soc. *133*, 1678–1681.

Fors, B.P., and Hawker, C.J. (2012). Control of a living radical polymerization of methacrylates by light. Angew. Chem. Int. Ed. *51*, 8850–8853.

Gibney, K.A., Sovadinova, I., Lopez, A.I., Urban, M., Ridgway, Z., Caputo, G.A., and Kuroda, K. (2012). Poly(ethylene imine)s as antimicrobial agents with selective activity. Macromol. Biosci. *12*, 1279–1289.

Goldberg, M., Mahon, K., and Anderson, D. (2008). Combinatorial and rational approaches to polymer synthesis for medicine. Adv. Drug Deliver. Rev. *60*, 971–978.

Gormley, A.J., Yeow, J., Ng, G., Conway, O., Boyer, C., and Chapman, R. (2018). An oxygen-tolerant PET-RAFT polymerization for screening structure-activity relationships. Angew. Chem. Int. Ed. *57*, 1557–1562.

Gregg, R.A., and Mayo, F.R. (1947). Chain transfer in the polymerisation of styrene iii. The reactivities of hydrocarbons toward the styrene radical. Discuss. Faraday Soc. *2*, 328–342.

Gupta, N., Lin, B.F., Campos, L., Dimitriou, M.D., Hikita, S.T., Treat, N.D., Tirrell, M.V., Clegg, D.O., Kramer, E.J., and Hawker, C.J. (2010). A versatile approach to high-throughput microarrays using thiol-ene chemistry. Nat. Chem. *2*, 138–145.

Gyawali, R., and Ibrahim, S.A. (2014). Natural products as antimicrobial agents. Food Control *46*, 412–429.

Hanak, J.J. (1970). Multiple-sample-concept in materials research - synthesis, compositional analysis and testing of entire multicomponent systems. J. Mater. Sci. *5*, 964–971.

Hantzsch, A. (1881). Condensationprodukte aus Aldehydammoniak und Ketonartigen Verbindungen. Ber. Dtsch. Chem. Ges. *14*, 1637–1638.

Hook, A.L., Chang, C.Y., Yang, J., Luckett, J., Cockayne, A., Atkinson, S., Mei, Y., Bayston, R., Irvine, D.J., Langer, R., et al. (2012). Combinatorial discovery of polymers resistant to bacterial attachment. Nat. Biotechnol. *30*, 868–875.

Judzewitsch, P.R., Nguyen, T.K., Shanmugam, S., Wong, E.H.H., and Boyer, C. (2018). Towards sequence-controlled antimicrobial polymers: effect of polymer block order on antimicrobial activity. Angew. Chem. Int. Ed. *57*, 4559–4564.

Kakuchi, R., and Theato, P. (2014). Efficient multicomponent postpolymerization modification based on kabachnik-fields reaction. ACS Macro. Lett. *3*, 329–332.

Khan, F., Tare, R.S., Kanczler, J.M., Oreffo, R.O.C., and Bradley, M. (2010). Strategies for cell manipulation and skeletal tissue engineering using high-throughput polymer blend formulation and microarray techniques. Biomaterials *31*, 2216–2228.

Kreye, O., Toth, T., and Meier, M.A.R. (2011). Introducing multicomponent reactions to polymer science: Passerini reactions of renewable monomers. J. Am. Chem. Soc. *133*, 1790–1792.

Kuroki, A., Sangwan, P., Qu, Y., Peltier, R., Sanchez-Cano, C., Moat, J., Dowson, C.G., Williams, E.G.L., Locock, K.E.S., Hartlieb, M., et al. (2017). Sequence control as a powerful tool for improving the selectivity of antimicrobial polymers. ACS Appl. Mater. Interface *9*, 40117–40126.

Lam, S.J., O'Brien-Simpson, N.M., Pantarat, N., Sulistio, A., Wong, E.H.H., Chen, Y.Y., Lenzo, J.C., Holden, J.A., Blencowe, A., Reynolds, E.C., et al. (2016). Combating multidrug-resistant Gram-negative bacteria with structurally nanoengineered antimicrobial peptide polymers. Nat. Microbiol. *1*, 16162.

Lee, I.H., Kim, H., and Choi, T.L. (2013). Cu-catalyzed multicomponent polymerization to synthesize a library of poly(N-sulfonylamidines). J. Am. Chem. Soc. *135*, 3760–3763.

Lehn, J.M., and Eliseev, A.V. (2001). Chemistry - dynamic combinatorial chemistry. Science *291*, 2331–2332.

Liu, Y.J., Gao, M., Lam, J.W.Y., Hu, R.R., and Tang, B.Z. (2014). Copper-catalyzed polycoupling of diynes, primary amines, and aldehydes: a new one-pot multicomponent polymerization tool to functional polymers. Macromolecules *47*, 4908–4919.

Llevot, A., Boukis, A.C., Oelmann, S., Wetzel, K., and Meier, M.A.R. (2017). An update on isocyanide-based multicomponent reactions in polymer science. Top. Curr. Chem. *375*, 127–155.

Loev, B., Goodman, M.M., Snader, K.M., Tedeschi, R., and Macko, E. (1974). Hantzsch-type dihydropyridine hypotensive agents .3. J. Med. Chem. *17*, 956–965.

Lynn, D.M., Anderson, D.G., Putnam, D., and Langer, R. (2001). Accelerated discovery of synthetic transfection vectors: parallel synthesis and screening of degradable polymer library. J. Am. Chem. Soc. *123*, 8155–8156.

Mao, T.F., Liu, G.Q., Wu, H.B., Wei, Y., Gou, Y.Z., Wang, J., and Tao, L. (2018). High throughput preparation of UV-protective polymers from essential oil extracts via the Biginelli reaction. J. Am. Chem. Soc. *140*, 6865–6872.

Mei, Y., Saha, K., Bogatyrev, S.R., Yang, J., Hook, A.L., Kalcioglu, Z.I., Cho, S.W., Mitalipova, M., Pyzocha, N., Rojas, F., et al. (2010). Combinatorial development of biomaterials for clonal growth of

human pluripotent stem cells. Nat. Mater. *9*, 768–778.

Meier, M.A.R., Gohy, J.F., Fustin, C.A., and Schubert, U.S. (2004a). Combinatorial synthesis of star-shaped block copolymers: host-guest chemistry of unimolecular reversed micelles. J. Am. Chem. Soc. *126*, 11517–11521.

Meier, M.A.R., Hoogenboom, R., and Schubert, U.S. (2004b). Combinatorial methods, automated synthesis and high-throughput screening in polymer research: the evolution continues. Macromol. Rapid Commun. *25*, 21–33.

Morimatsu, K., Eguchi, K., Hamanaka, D., Tanaka, F., and Uchino, T. (2012). Effects of temperature and nutrient conditions on biofilm formation of *Pseudomonas putida*. Food Sci. Technol. Res. *18*, 879–883.

Namivandi-Zangeneh, R., Kwan, R.J., Nguyen, T.K., Yeow, J., Byrne, F.L., Oehlers, S.H., Wong, E.H.H., and Boyer, C. (2018). The effects of polymer topology and chain length on the antimicrobial activity and hemocompatibility of amphiphilic ternary copolymers. Polym. Chem. *9*, 1735–1744.

Neumann, K., Conde-Gonzalez, A., Owens, M., Venturato, A., Zhang, Y.C., Geng, J., and Bradley, M. (2017). An approach to the high-throughput fabrication of glycopolymer microarrays through thiol-ene chemistry. Macromolecules *50*, 6026–6031.

Okamura, S., and Katagiri, K. (1958). Chain transfer to telomer. Makromolekul. Chem. *28*, 177–184.

Rademann, J., and Jung, G. (2000). Drug discovery - integrating combinatorial synthesis and bioassays. Science *287*, 1947–1948.

Rosen, B.M., and Percec, V. (2009). Single-electron transfer and single-electron transfer degenerative chain transfer living radical polymerization. Chem. Rev. *109*, 5069–5119.

Sehlinger, A., Kreye, O., and Meier, M.A.R. (2013). Tunable polymers obtained from Passerini multicomponent reaction derived acrylate monomers. Macromolecules *46*, 6031–6037.

Siamaki, A.R., Sakalauskas, M., and Arndtsen, B.A. (2011). A palladium-catalyzed multicomponent coupling approach to pi-conjugated oligomers: assembling imidazole-based materials from imines and acyl chlorides. Angew. Chem. Int. Ed. *50*, 6552–6556.

Steinberger, R.E., Allen, A.R., Hansma, H.G., and Holden, P.A. (2002). Elongation correlates with nutrient deprivation in *Pseudomonas aeruginosa*-unsaturated biofilms. Microb. Ecol. *43*, 416–423.

Stout, D.M., and Meyers, A.I. (1982). Recent advances in the chemistry of dihydropyridines. Chem. Rev. *82*, 223–243.

Theato, P. (2015). Multi-Component and Sequential Reactions in Polymer Synthesis, *Vol. 269* (Springer).

Ting, J.M., Nayale, T.S., Jones, S.D., Bates, F.S., and Reineke, T.M. (2015). Deconstructing HPMCAS: excipient design to tailor polymer-drug interactions for oral drug delivery. ACS Biomater. Sci. Eng. *1*, 978–990.

Ting, J.M., Tale, S., Purchel, A.A., Jones, S.D., Widanapathirana, L., Tolstyka, Z.P., Guo, L., Guillaudeu, S.J., Bates, F.S., and Reineke, T.M. (2016). High-throughput excipient discovery enables oral delivery of poorly soluble pharmaceuticals. ACS Cent. Sci. *2*, 748–755.

Vijesh, A.M., Isloor, A.M., Peethambar, S.K., Shivananda, K.N., Arulmoli, T., and Isloor, N.A. (2011). Hantzsch reaction: synthesis and characterization of some new 1,4-dihydropyridine derivatives as potent antimicrobial and antioxidant agents. Eur. J. Med. Chem. *46*, 5591–5597.

Wu, H.B., Wang, Z.M., and Tao, L. (2017a). The Hantzsch reaction in polymer chemistry: synthesis and tentative application. Polym. Chem. *8*, 7290–7296.

Wu, H.B., Yang, L., and Tao, L. (2017b). Polymer synthesis by mimicking nature's strategy: the combination of ultra-fast RAFT and the Biginelli reaction. Polym. Chem. *8*, 5679–5687.

Xiang, X.D., Sun, X.D., Briceno, G., Lou, Y.L., Wang, K.A., Chang, H.Y., Wallacefreedman, W.G., Chen, S.W., and Schultz, P.G. (1995). A combinatorial approach to materials discovery. Science *268*, 1738–1740.

Xu, J.T., Shanmugam, S., Fu, C.K., Aguey-Zinsou, K.F., and Boyer, C. (2016). Selective photoactivation: from a single unit monomer insertion reaction to controlled polymer architectures. J. Am. Chem. Soc. *138*, 3094–3106.

Xue, H.D., Zhao, Y., Wu, H.B., Wang, Z.L., Yang, B., Wei, Y., Wang, Z.M., and Tao, L. (2016). Multicomponent combinatorial polymerization via the Biginelli reaction. J. Am. Chem. Soc. *138*, 8690–8693.

Yang, B., Zhao, Y., Ren, X., Zhang, X.Y., Fu, C.K., Zhang, Y.L., Wei, Y., and Tao, L. (2015). The power of one-pot: a hexa-component system containing pi-pi stacking, Ugi reaction and RAFT polymerization for simple polymer conjugation on carbon nanotubes. Polym. Chem. *6*, 509–513.

Zhang, Q., Wilson, P., Li, Z.D., McHale, R., Godfrey, J., Anastasaki, A., Waldron, C., and Haddleton, D.M. (2013). Aqueous copper-mediated living polymerization: exploiting rapid disproportionation of CuBr with Me6TREN. J. Am. Chem. Soc. *135*, 7355–7363.

Zhang, Q.D., Zhang, Y.L., Zhao, Y., Yang, B., Fu, C.K., Wei, Y., and Tao, L. (2015). Multicomponent polymerization system combining Hantzsch reaction and reversible addition-fragmentation chain transfer to efficiently synthesize well-defined poly(1,4-dihydropyridine)s. ACS Macro. Lett. *4*, 128–132.

Zhang, X.J., Wang, S.X., Liu, J., Xie, Z.G., Luan, S.F., Xiao, C.S., Tao, Y.H., and Wang, X.H. (2016). Ugi reaction of natural amino acids: a general route toward facile synthesis of polypeptoids for bioapplications. ACS Macro. Lett. *5*, 1049–1054.

Zhang, Y.L., Zhao, Y., Yang, B., Zhu, C.Y., Wei, Y., and Tao, L. (2014). 'One pot' synthesis of well-defined poly(aminophosphonate)s: time for the Kabachnik-Fields reaction on the stage of polymer chemistry. Polym. Chem. *5*, 1857–1862.

Zhao, Y., Wu, H.B., Wang, Z.L., Wei, Y., Wang, Z.M., and Tao, L. (2016). Training the old dog new tricks: the applications of the Biginelli reaction in polymer chemistry. Sci. China. Chem. *59*, 1541–1547.

Zhu, C.Y., Yang, B., Zhao, Y.A., Fu, C.K., Tao, L., and Wei, Y. (2013). A new insight into the Biginelli reaction: the dawn of multicomponent click chemistry? Polym. Chem. *4*, 5395–5400.

ISCI, Volume *23*

Supplemental Information

High-Throughput Preparation of Antibacterial Polymers from Natural Product Derivatives via the Hantzsch Reaction

Guoqiang Liu, Qiang Zhang, Yongsan Li, Xing Wang, Haibo Wu, Yen Wei, Yuan Zeng, and Lei Tao

Supporting Data

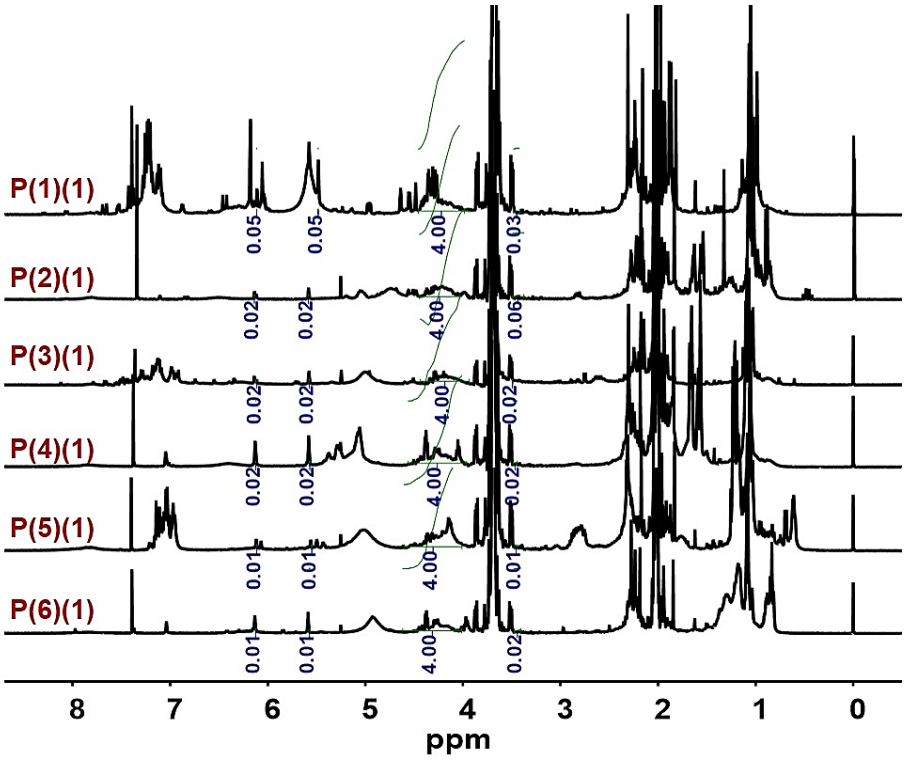

Figure S1. ^{1}H NMR spectra ($CDCl_3$, 400M) of crude **P(X)(1)** after HTP polymerization for conversion calculation. Related to Figure 1.

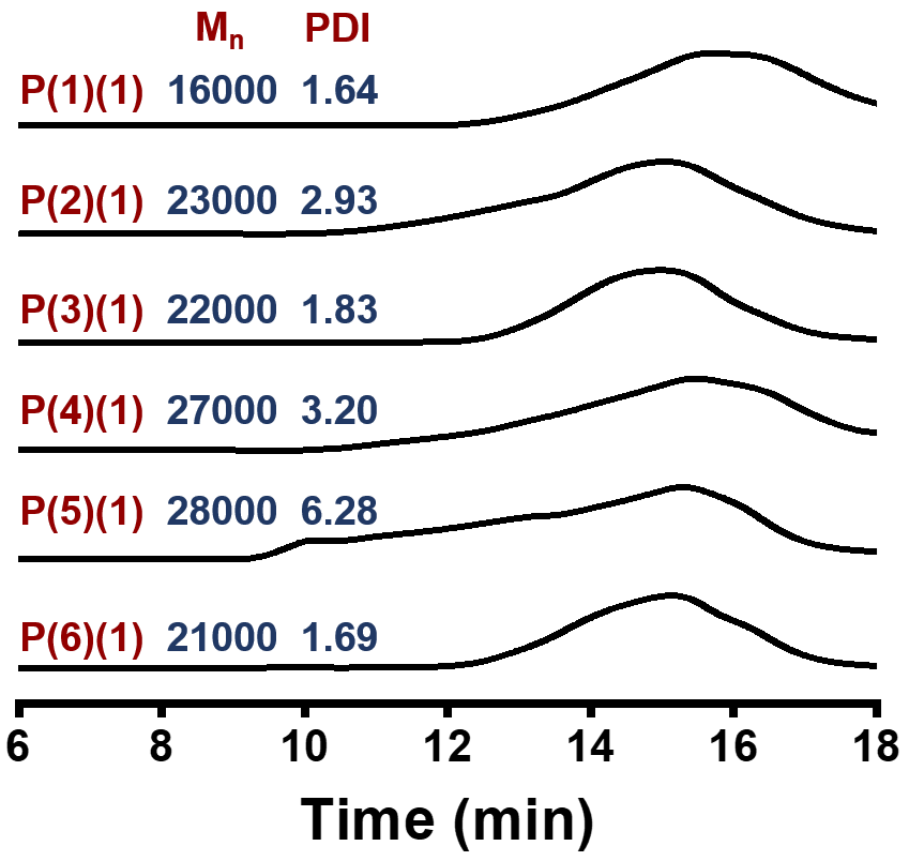

Figure S2. GPC traces of **P(X)(1)**. Related to Figure 1.

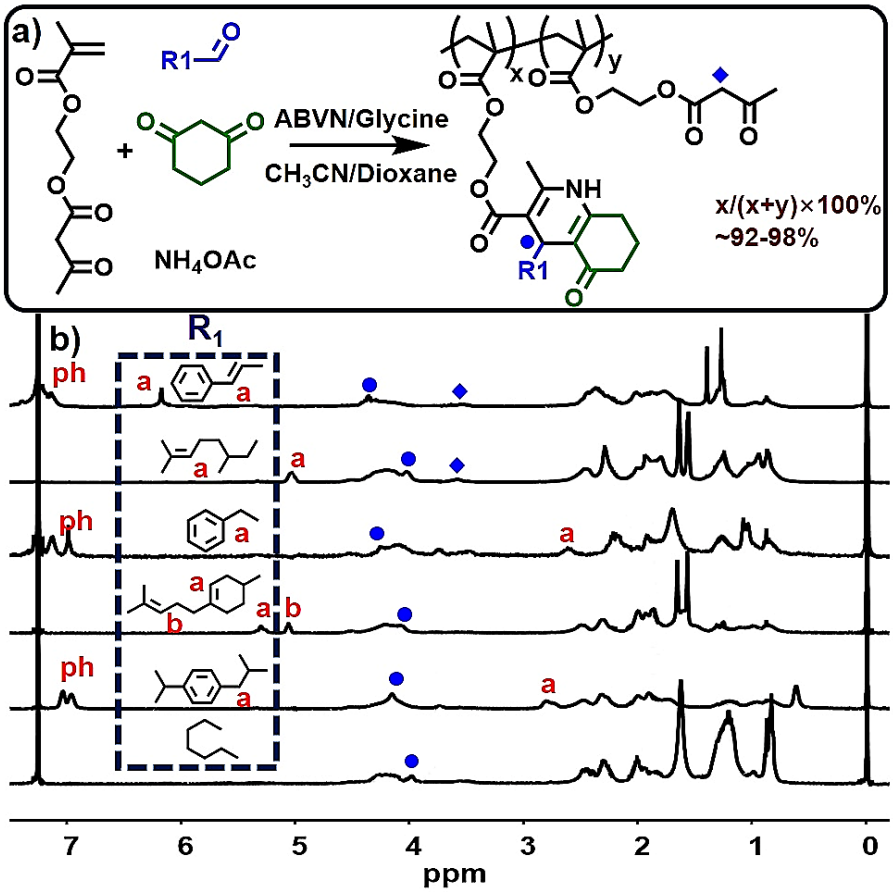

Figure S3. a) Reaction conditions: acetonitrile/dioxane (1/1, v/v) as the solvent, glycine (10% to aldehyde) as the Hantzsch reaction catalyst, ABVN (2% to AEMA) as the initiator for FRP, 75°C, and 12 h. **A(X)**: **B(2)**: AEMA: NH_4OAc = 1:1:1:1.5. b) ^1H NMR spectra ($CDCl_3$, 400M) of **P(X)(2)**. Related to Figure 1.

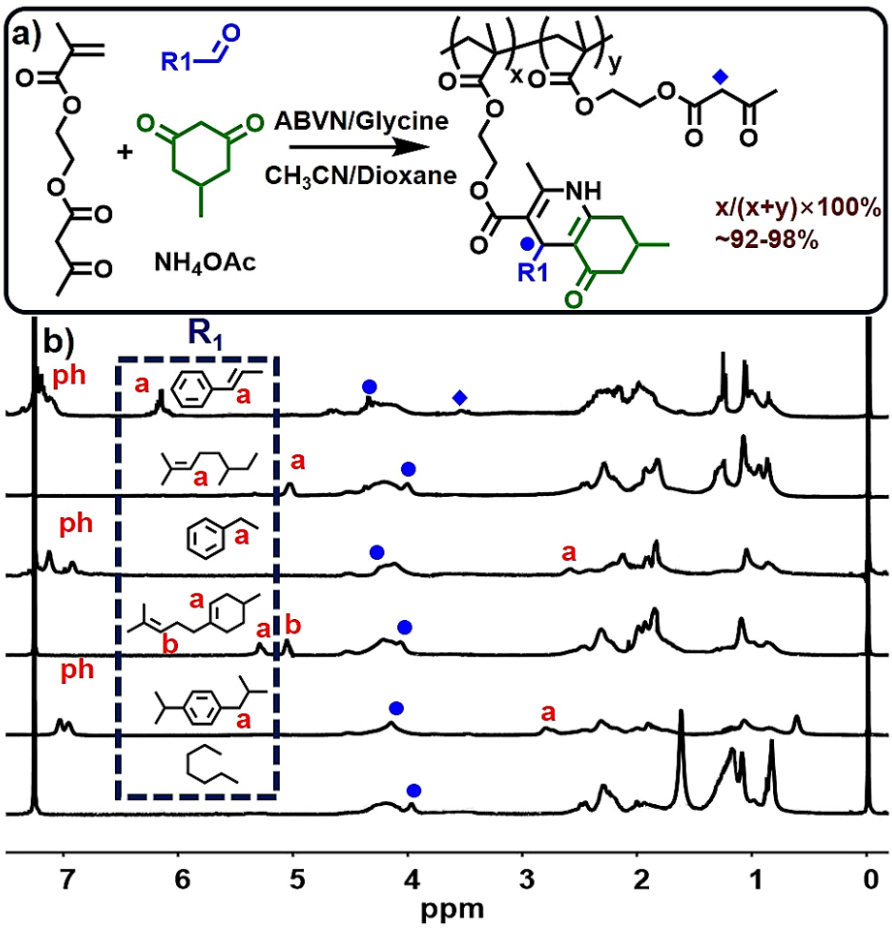

Figure S4. a) Reaction conditions: acetonitrile/dioxane (1/1, v/v) as the solvent, glycine (10% to aldehydes) as the Hantzsch reaction catalyst, ABVN (2% to AEMA) as the initiator for FRP, 75°C, and 12 h. **A(X)**: **B(3)**: AEMA: NH4OAc = 1:1:1:1.5. b) ^{1}H NMR spectra ($CDCl_3$, 400M) of **P(X)(3)**. Related to Figure 1.

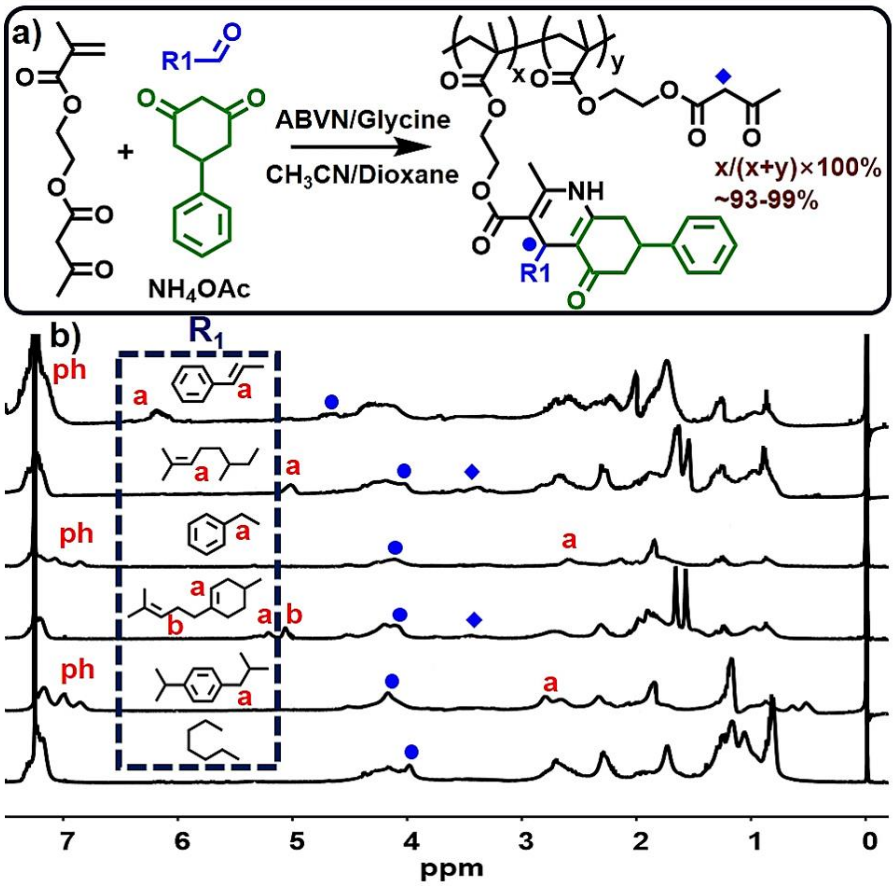

Figure S5. a) Reaction conditions: acetonitrile/dioxane (1/1, v/v) as the solvent, glycine (10% to aldehyde) as the Hantzsch reaction catalyst, ABVN (2% to AEMA) as the initiator for FRP, 75°C, and 12 h. **A(X)**: **B(4)**: AEMA: NH_4OAc = 1:1:1:1.5. b) ^1H NMR spectra ($CDCl_3$, 400M) of **P(X)(4)**. Related to Figure 1.

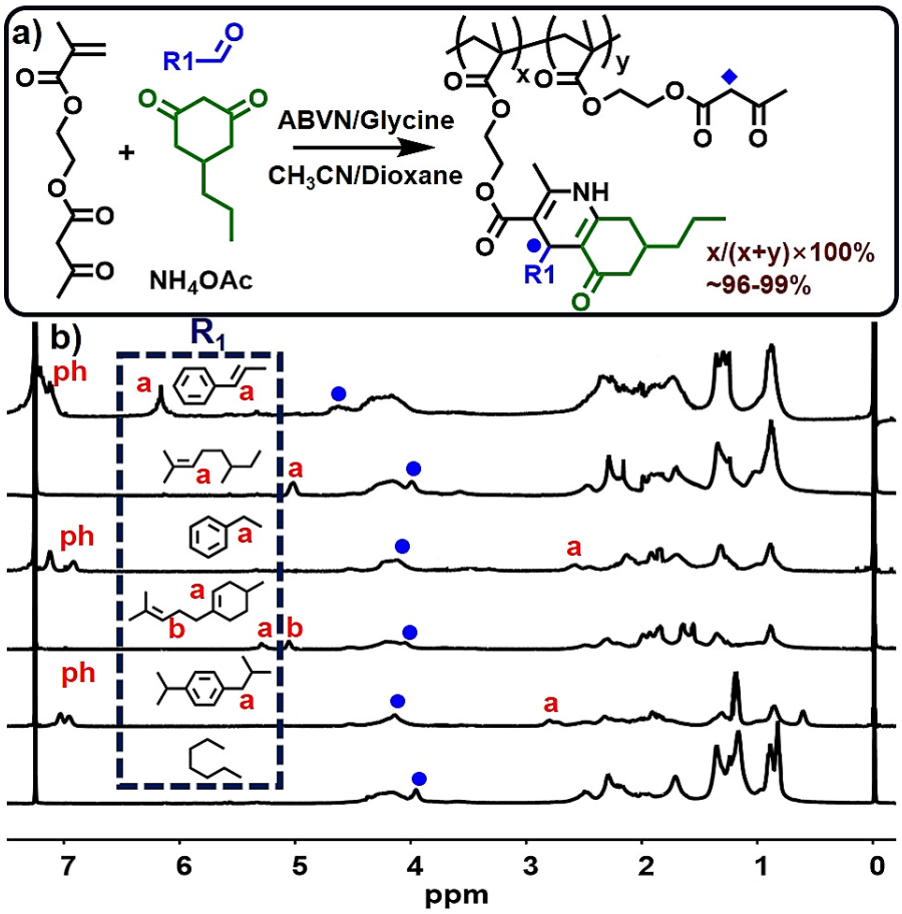

Figure S6. a) Reaction conditions: acetonitrile/dioxane (1/1, v/v) as the solvent, glycine (10% to aldehyde) as the Hantzsch reaction catalyst, ABVN (2% to AEMA) as the initiator for FRP, 75°C, and 12 h. **A(X)**: **B(5)**: AEMA: NH_4OAc = 1:1:1:1.5. b) ^1H NMR spectra ($CDCl_3$, 400M) of **P(X)(5)**. Related to Figure 1.

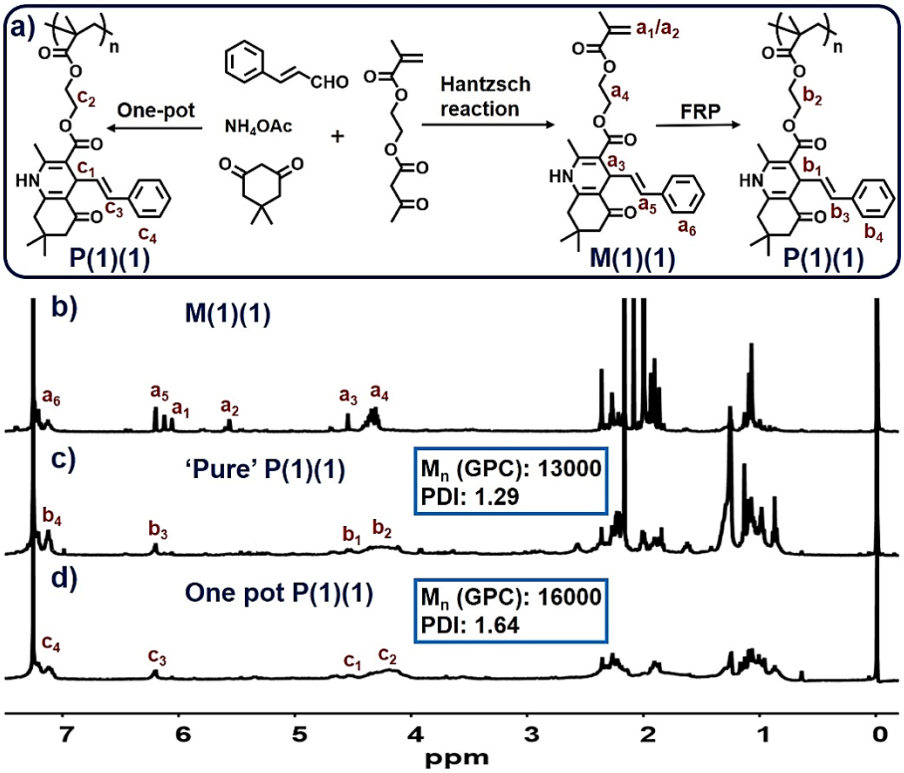

Figure S7. a) Preparations of **P(1)(1)** from the traditional monomer−polymer method and one-pot strategy. ^{1}H NMR spectra ($CDCl_3$, 400M) of b) **M(1)(1)**, c) "pure" **P(1)(1)**, and d) **P(1)(1)** *via* the one-pot Hantzsch−FRP method. Related to Figure 1.

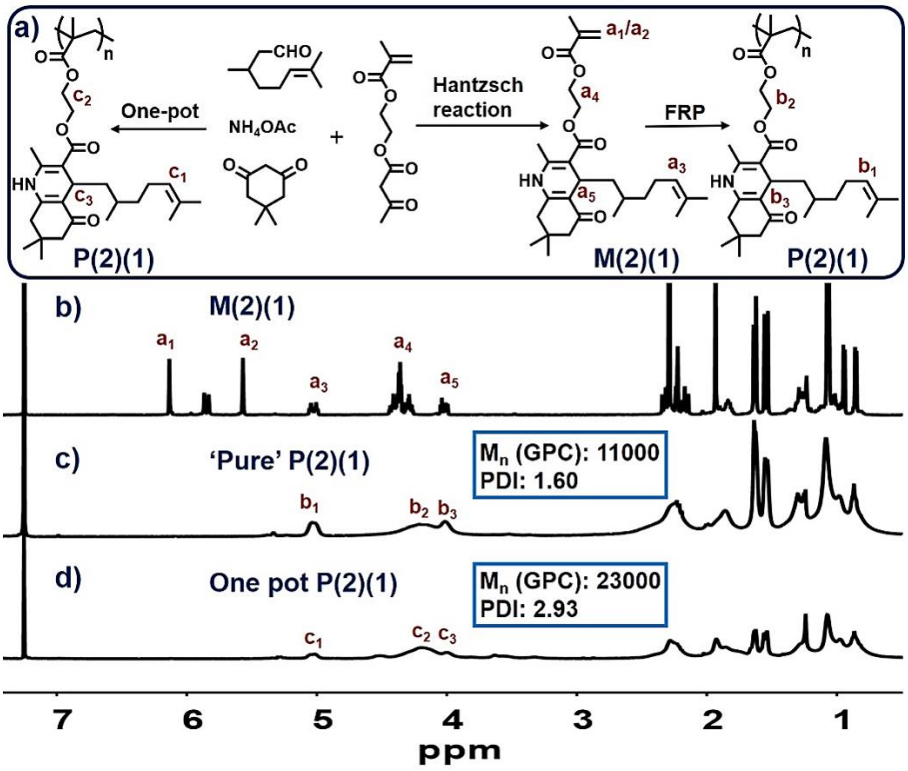

Figure S8. a) Preparations of **P(2)(1)** from the traditional monomer−polymer method and one-pot strategy. ^{1}H NMR spectra ($CDCl_3$, 400M) of b) **M(2)(1)**, c) "pure" **P(2)(1)**, and d) **P(2)(1)** *via* the one-pot Hantzsch−FRP method. Related to Figure 1.

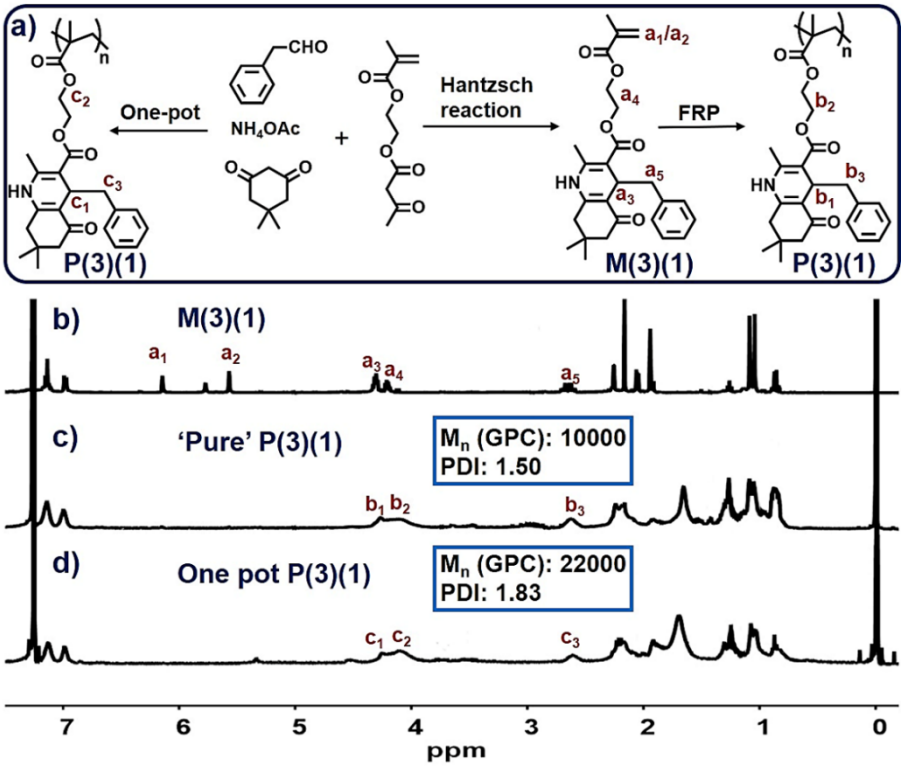

Figure S9. a) Preparations of **P(3)(1)** from the traditional monomer−polymer method and one-pot strategy. ^{1}H NMR spectra ($CDCl_3$, 400M) of b) **M(3)(1)**, c) "pure" **P(3)(1)**, and d) **P(3)(1)** *via* the one-pot Hantzsch−FRP method. Related to Figure 1.

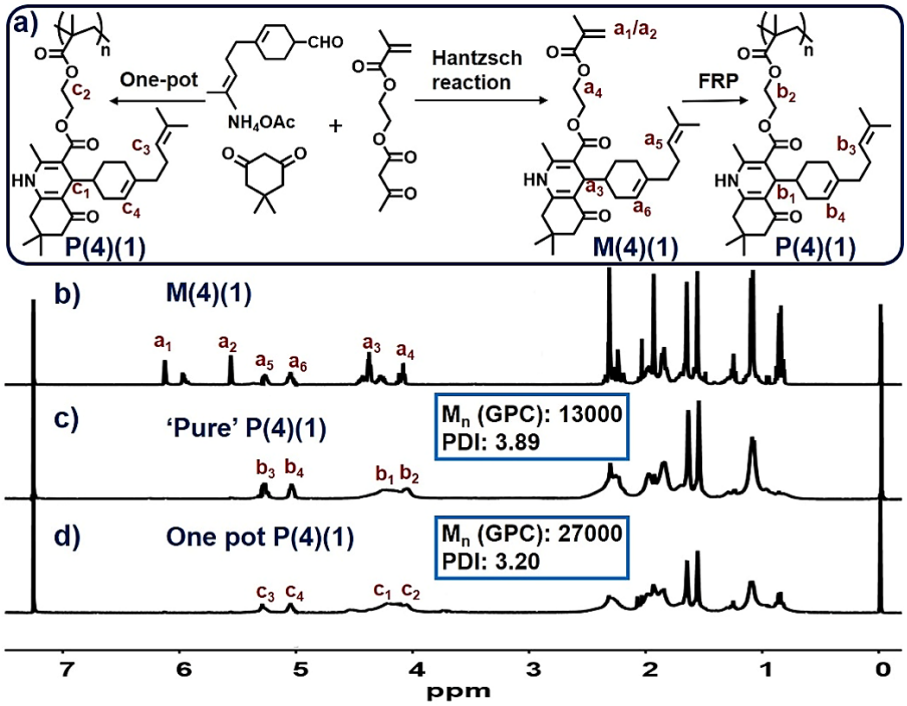

Figure S10. a) Preparations of **P(4)(1)** from the traditional monomer−polymer method and one-pot strategy. ^{1}H NMR spectra ($CDCl_3$, 400M) of b) **M(4)(1)**, c) "pure" **P(4)(1)**, and d) **P(4)(1)** *via* the one-pot Hantzsch−FRP method. Related to Figure 1.

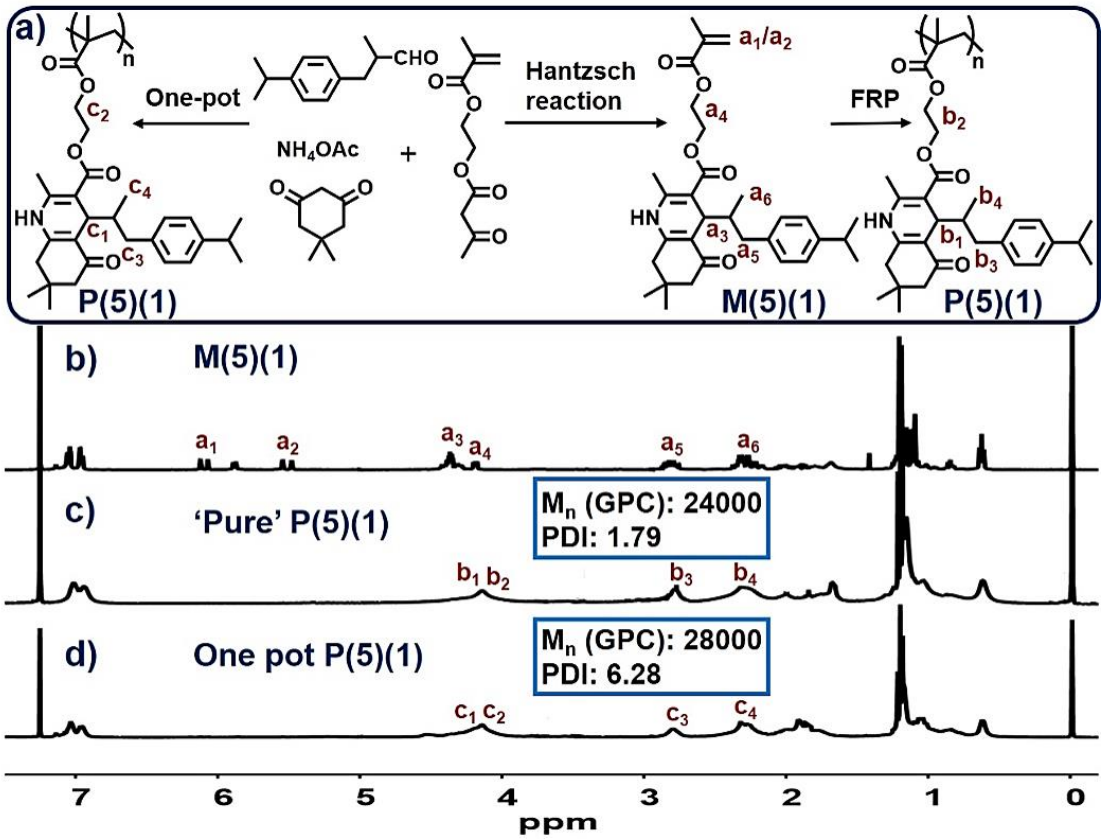

Figure S11. a) Preparations of **P(5)(1)** from the traditional monomer−polymer method and one-pot strategy. ^{1}H NMR spectra ($CDCl_3$, 400M) of b) **M(5)(1)**, c) "pure" **P(5)(1)**, and d) **P(5)(1)** *via* the one-pot Hantzsch−FRP method. Related to Figure 1.

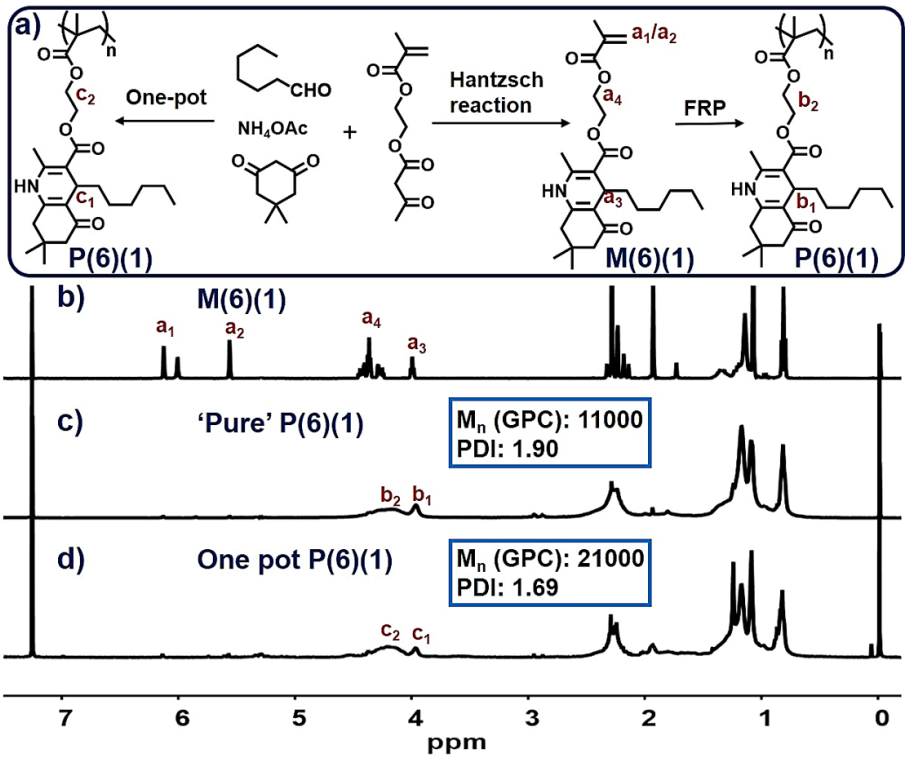

Figure S12. a) Preparations of **P(6)(1)** from the traditional monomer−polymer method and the one-pot strategy. ^{1}H NMR spectra of ($CDCl_3$, 400M) of b) **M(6)(1)**, c) "pure" **P(6)(1)**, and d) **P(6)(1)** *via* a one-pot Hantzsch−FRP system. Related to Figure 1.

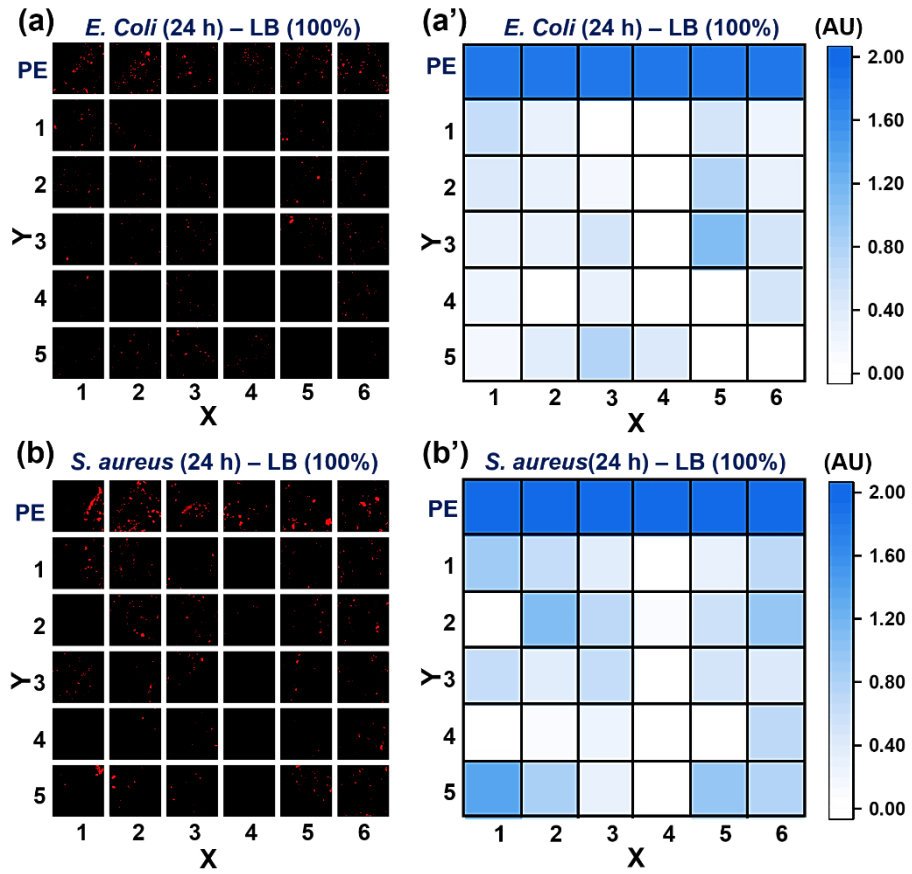

Figure S13. a) LSCM images and a') intensity map of *E. coli* on sample disks, 24 h, 100% LB medium. b) LSCM images and b') intensity map of *S. aureus* on sample disks, 24 h, 100% LB medium. Related to Figure 2.

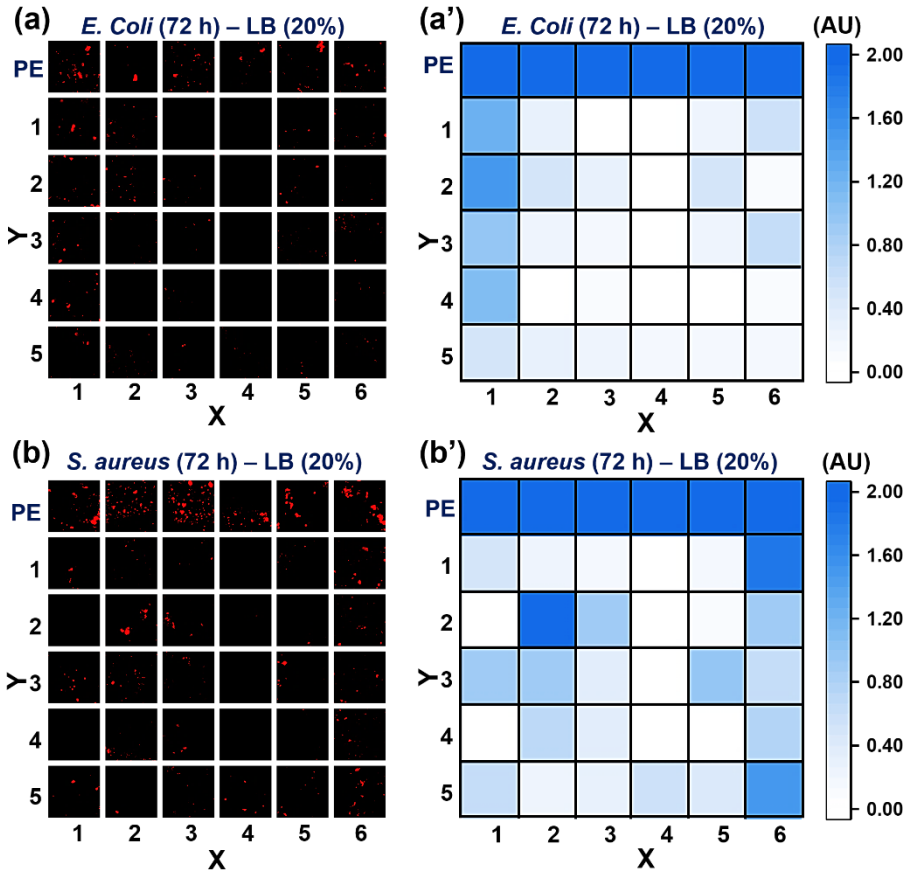

Figure S14. a) LSCM images and a') intensity map of *E. coli* on sample disks, 72 h, 20% LB medium. b) LSCM images and b') intensity map of *S. aureus* on sample disks, 72 h, 20% LB medium. Related to Figure 2.

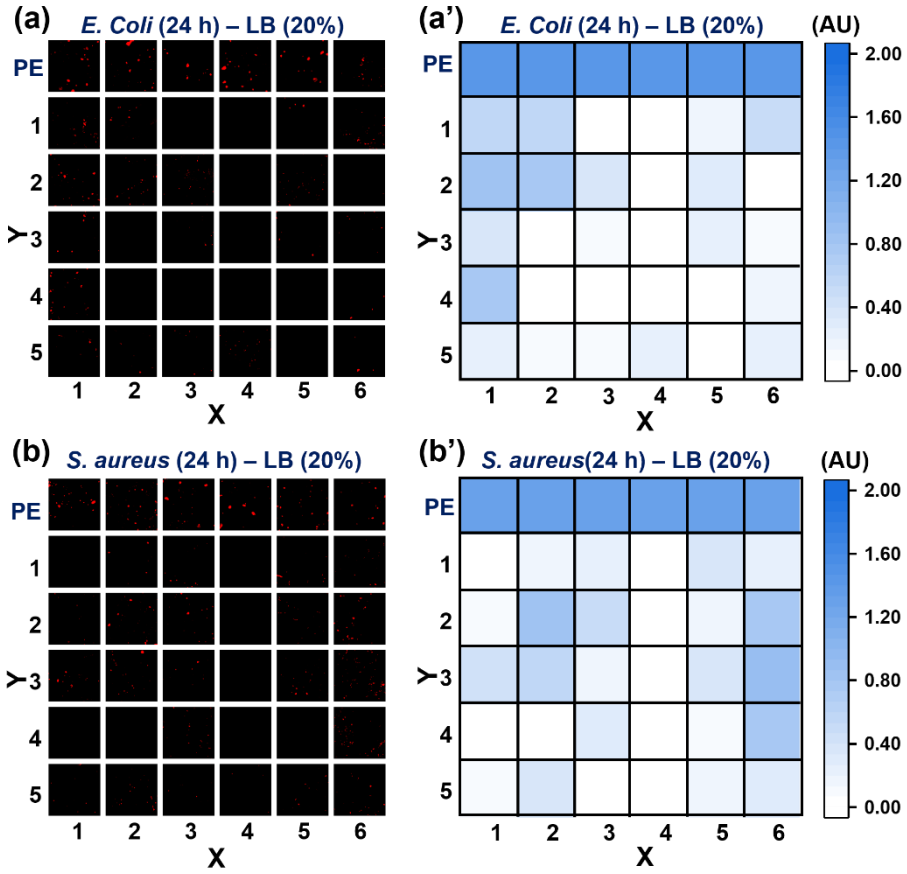

Figure S15. a) LSCM images and a') intensity map of *E. coli* on sample disks, 24 h, 20% LB medium. b) LSCM images and b') intensity map of *S. aureus* on sample disks, 24 h, 20% LB medium. Related to Figure 2.

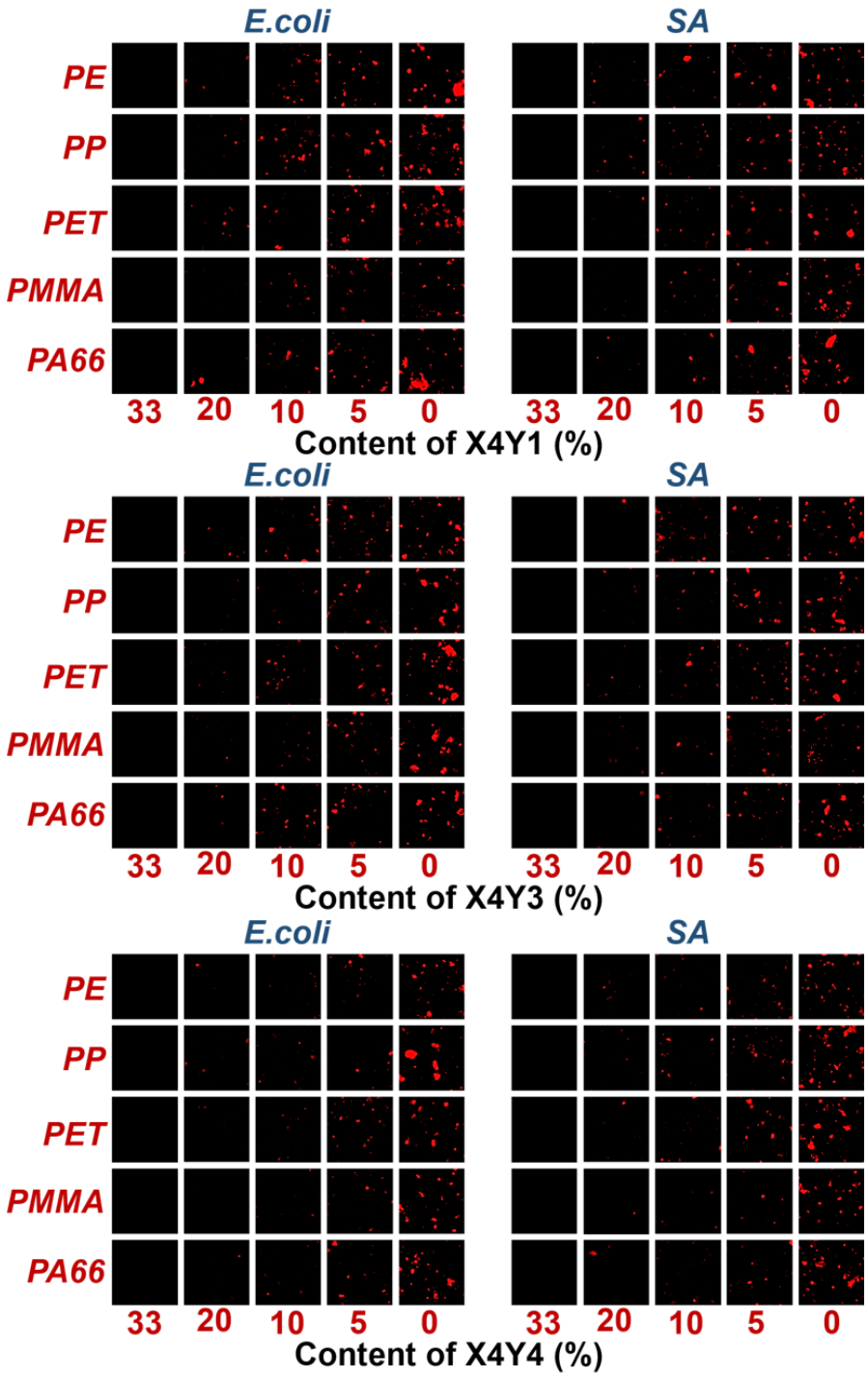

Figure S16. LSCM images of bacteria on sample disks after 72-h incubation in 100% LB medium. Three replicate samples were tested, commodity polymers served as the controls. a) Commodity polymers + **P(4)(1)**. b) Commodity polymers + **P(4)(3)**. c) Commodity polymers + **P(4)(4)**. Related to Figure 3.

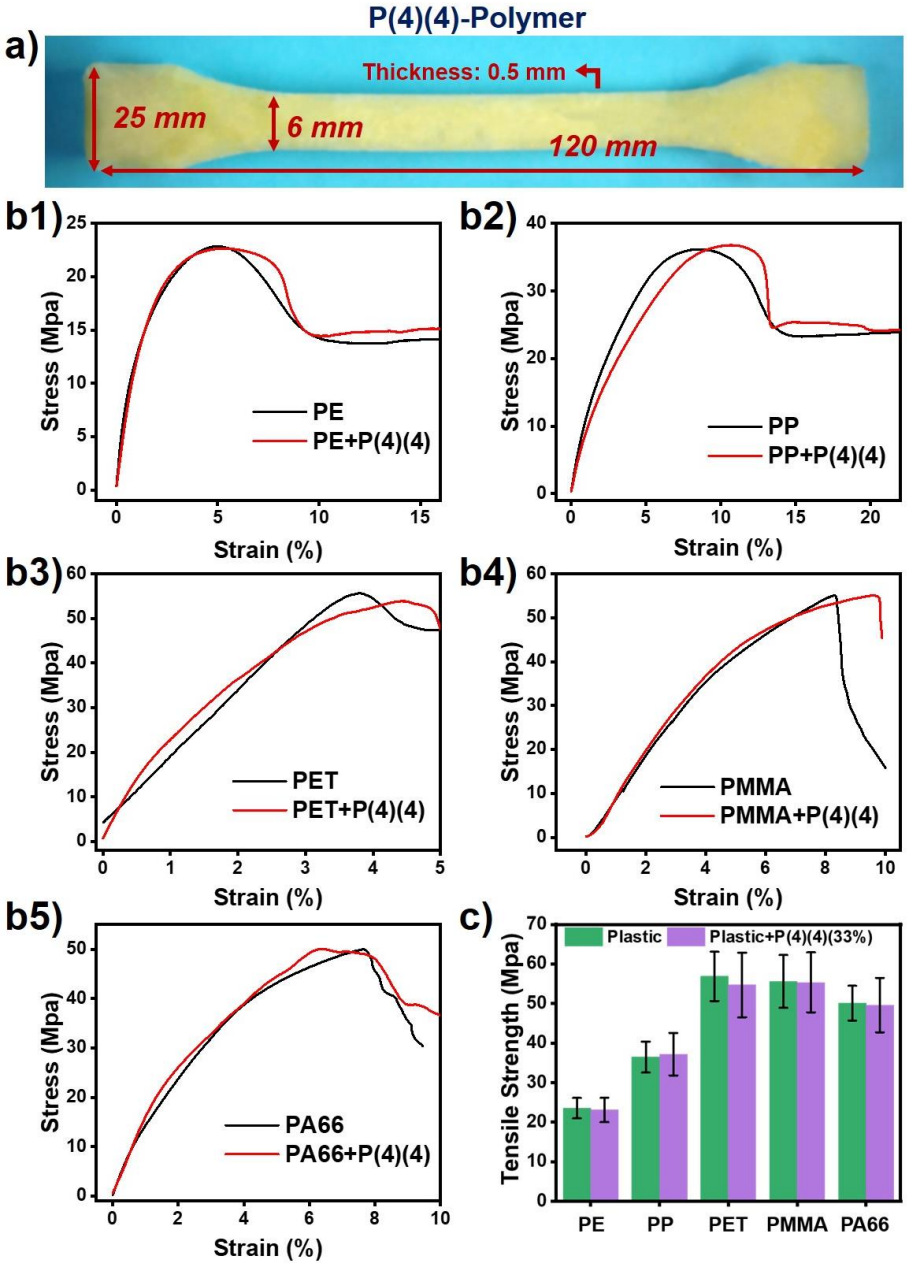

Figure S17. a) Typical samples of **P(4)(4)**-polymers. b1–5) Stress–strain curves of commodity polymers (black) and **P(4)(4)**-polymer blends (red). c) Tensile strength of commodity polymers and **P(4)(4)**-polymer blends. Data are represented as mean ± SD, n = 6. Related to Figure 4.

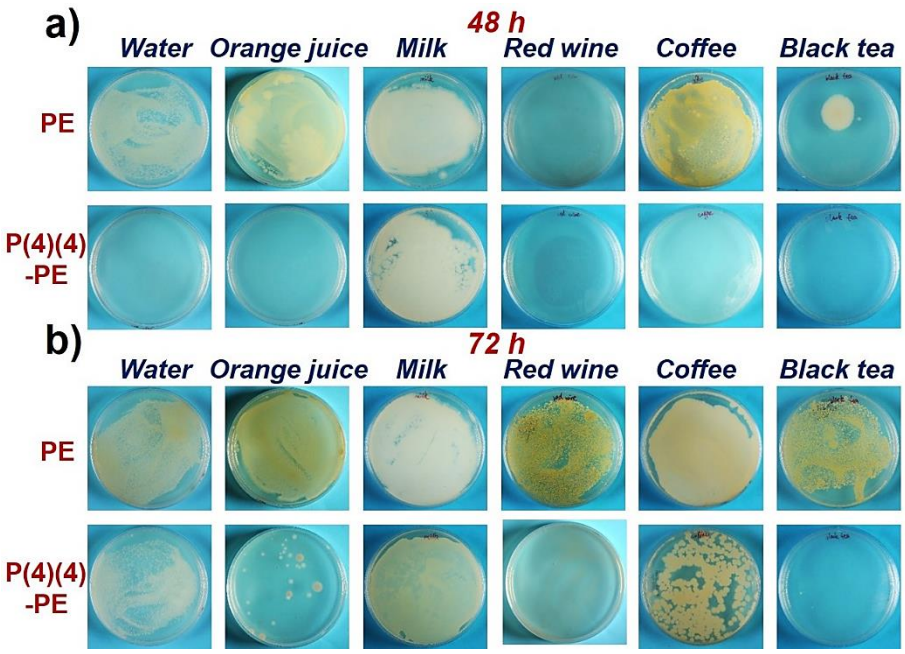

Figure S18. Images of the plate-streaking experiment: 100 μL sample on LB agar (diameter: 90 mm, thickness: 6 mm, LB: 1.5 g/L), a) 48 h culture, and b) 72 h culture. Related to Figure 4.

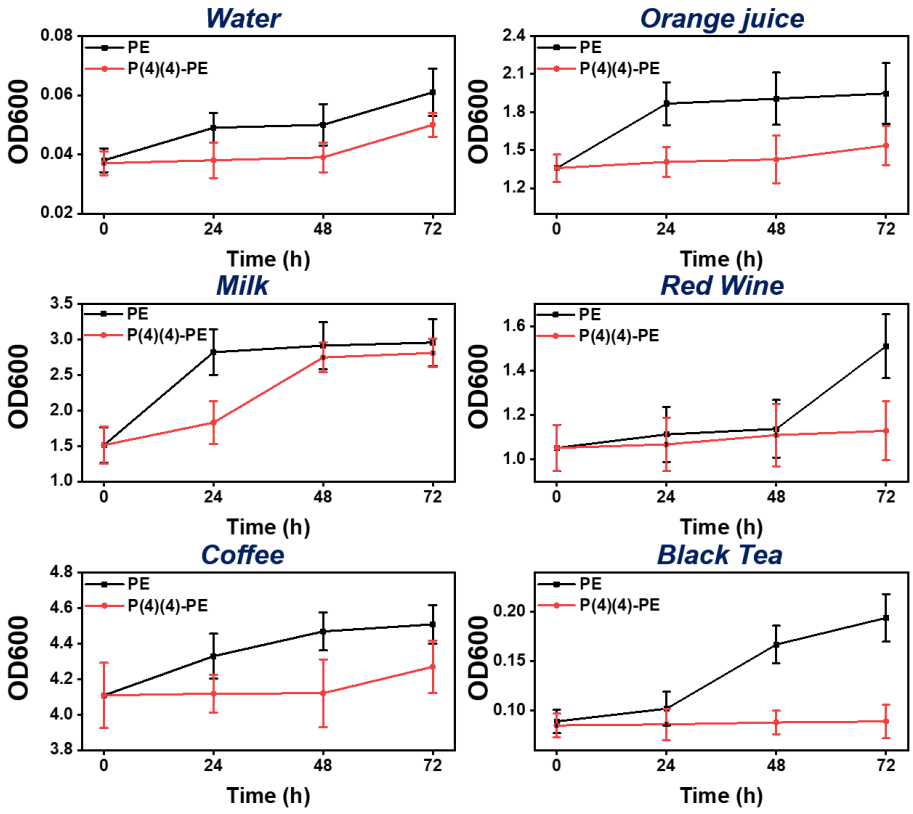

Figure S19. OD600 values versus time in the presence of different commercially available beverages. Data are represented as mean ± SD, n = 5. Related to Figure 4.

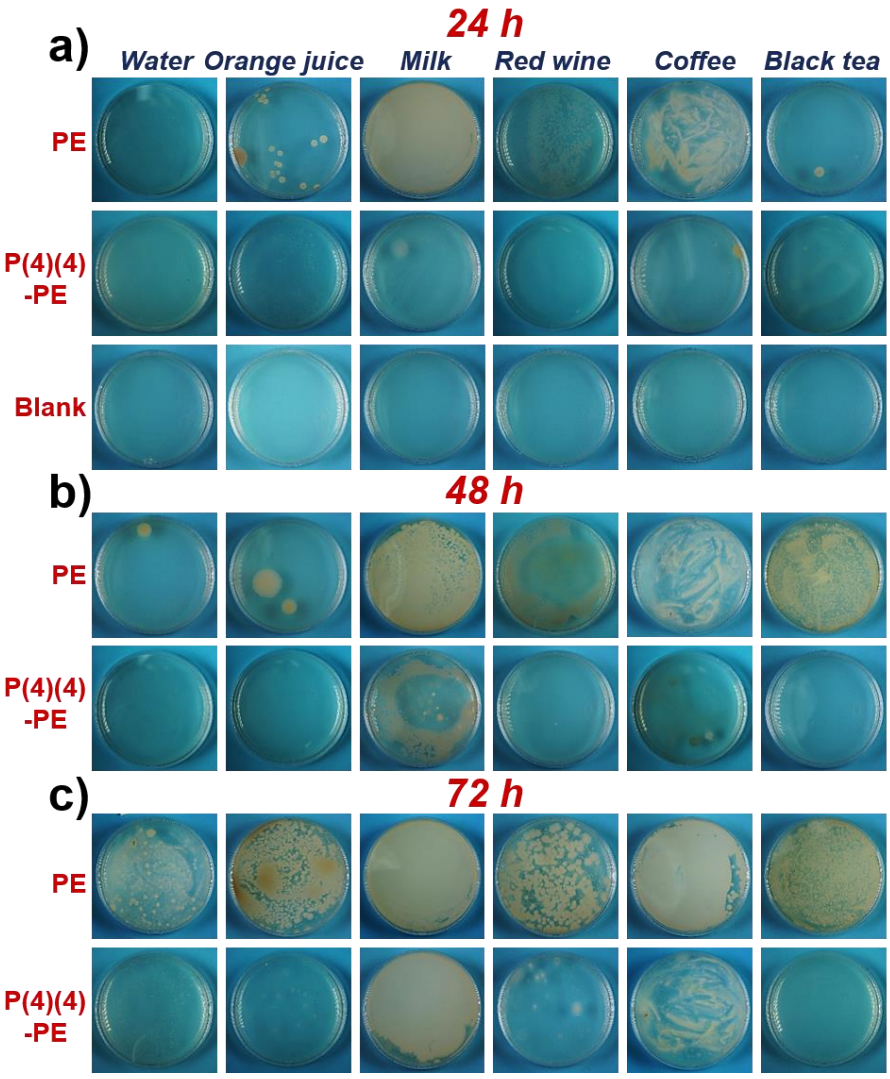

Figure S20. Images of the antibacterial capability test of bowls via a standard method. *S. aureus* was used as a model bacterium, 100 μL sample on LB agar (diameter: 90 mm, thickness: 6 mm, LB: 1.5 g/L). a) 24 h culture, b) 48 h culture and c) 72 h culture. Related to Figure 4.

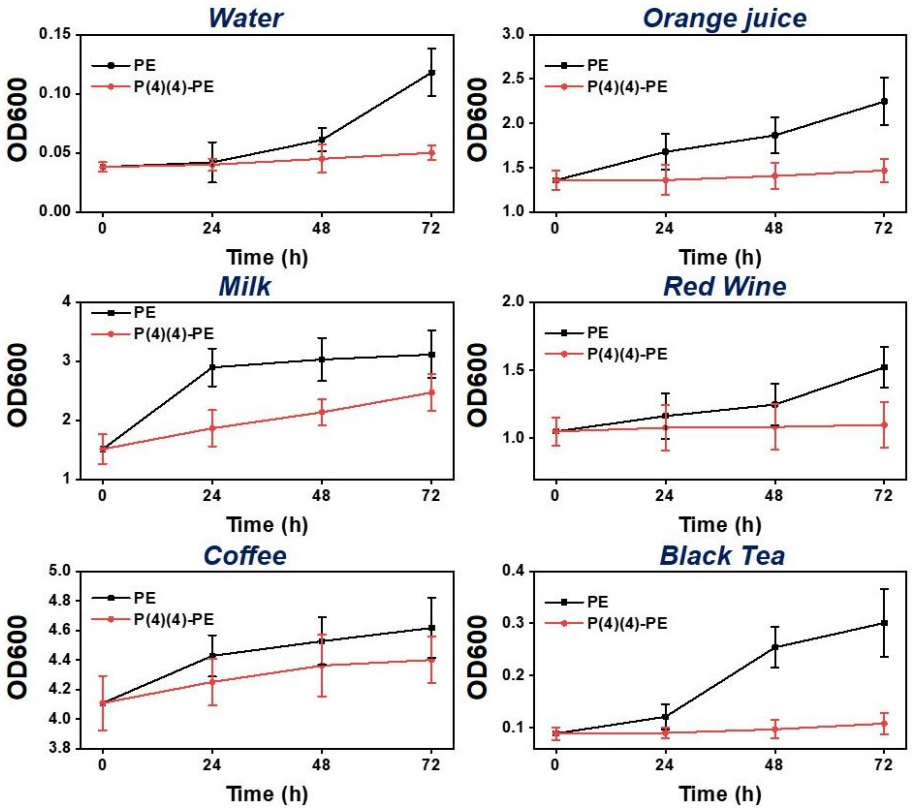

Figure S21. OD600 values versus time in the presence of different commercially available beverages in the standard antibacterial capability test of bowls, *S. aureus* was used as a model bacterium. Data are represented as mean ± SD, n = 5. Related to Figure 4.

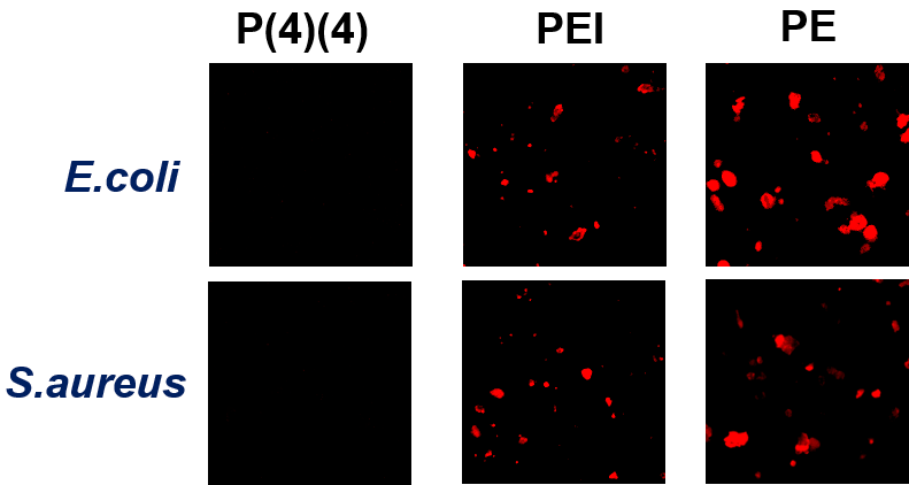

Figure S22. LSCM images of *E. coli* and *S. aureus* on sample disks after 72-h incubation. PE served as the control. Each image is 200 × 200 μm. Related to Figure 5.

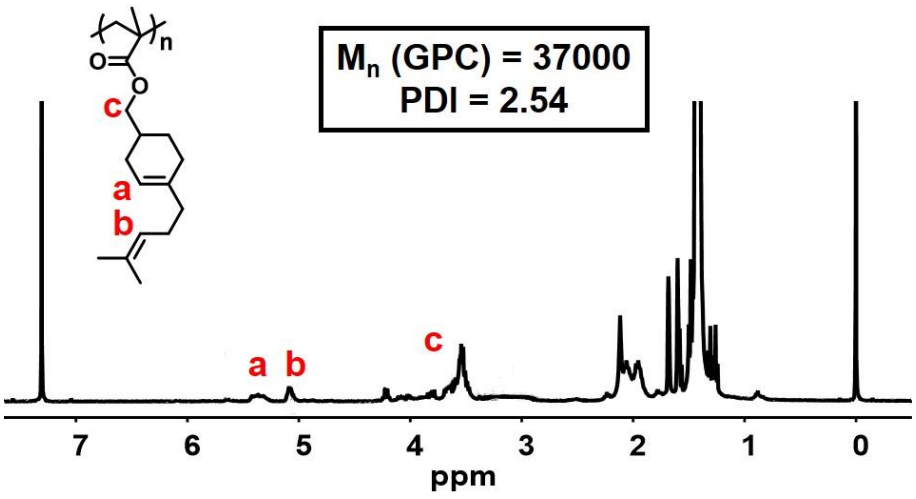

Figure S23. ^{1}H NMR spectrum ($CDCl_3$, 400M) of **P1**. Related to Figure 6.

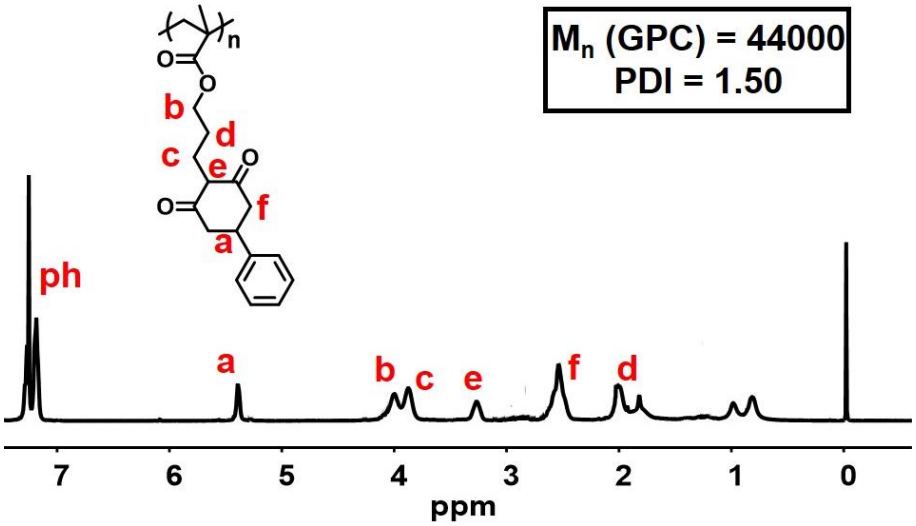

Figure S24. ^{1}H NMR spectrum ($CDCl_3$, 400M) of **P2**. Related to Figure 6.

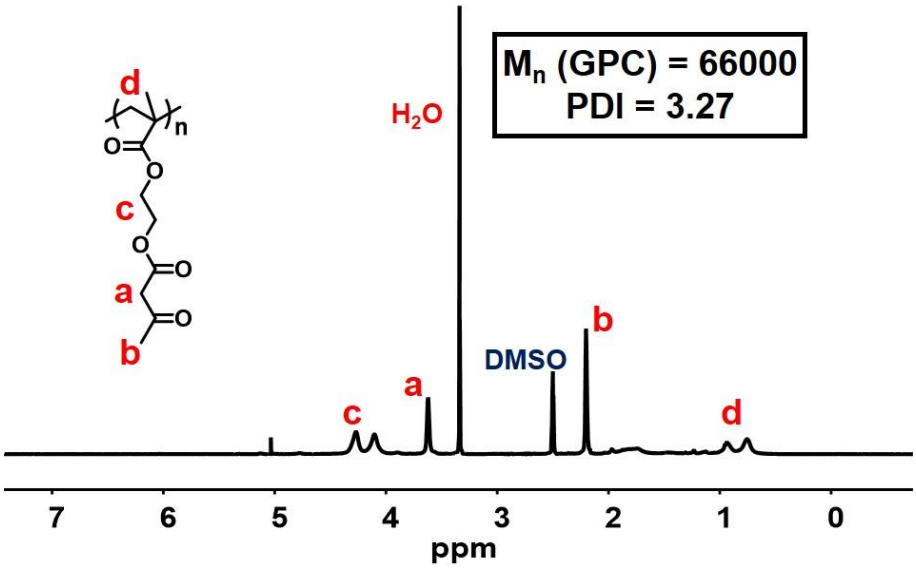

Figure S25. ^{1}H NMR spectrum (DMSO-d_6, 400M) of P(AEMA). Related to Figure 6.

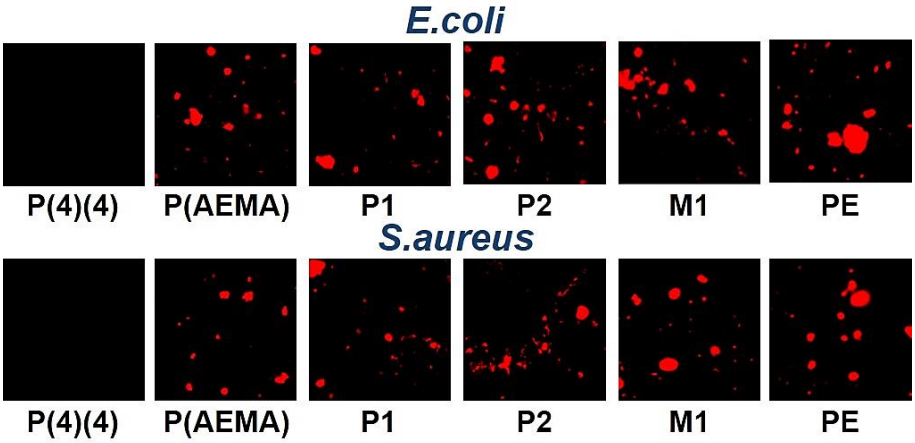

Figure S26. LSCM images of *E. coli* and *S. aureus* on sample disks after 72 h incubation. PE served as the control; each image is 200 × 200 μm. Related to Figure 6.

Table S1. The Hantzsch-type polymers (**P(X)(Y)**). Related to Figure 1.

Polymer	Conv.(vinyl)[a]	Conv.(Hantzsch)[a]	M_n[b]	PDI[b]	T_g[c](°C)	T_d[d](°C)
P(1)(1)	95%	97%	16000	1.64	115.4	207
P(2)(1)	98%	94%	23000	2.93	88.2	252
P(3)(1)	98%	98%	22000	1.83	102.6	232
P(4)(1)	98%	98%	27000	3.20	106.8	221
P(5)(1)	99%	99%	28000	6.28	111.3	227
P(6)(1)	99%	98%	21000	1.69	121.3	308
P(1)(2)	97%	95%	16000	1.39	90.6	228
P(2)(2)	97%	92%	19000	1.85	88.3	263
P(3)(2)	97%	93%	23000	1.96	98.7	251
P(4)(2)	98%	94%	28000	1.35	102.9	216
P(5)(2)	98%	95%	22000	3.42	105.7	226
P(6)(2)	99%	98%	19000	1.48	85.2	283
P(1)(3)	97%	93%	20000	1.48	117.2	208
P(2)(3)	96%	92%	24000	1.77	93.6	256
P(3)(3)	98%	93%	23000	2.14	105.6	236
P(4)(3)	99%	94%	30000	1.37	100.0	224
P(5)(3)	99%	95%	20000	3.35	108.9	267
P(6)(3)	98%	98%	22000	1.48	103.5	282
P(1)(4)	98%	93%	24000	1.26	112.6	237
P(2)(4)	98%	98%	25000	1.71	73.9	292
P(3)(4)	98%	98%	26000	1.94	97.9	219
P(4)(4)	97%	98%	23000	1.83	97.1	208
P(5)(4)	99%	99%	20000	2.30	103.6	268
P(6)(4)	99%	99%	26000	1.64	101.1	283
P(1)(5)	95%	97%	23000	1.47	56.6	246
P(2)(5)	96%	97%	21000	1.79	84.2	250
P(3)(5)	97%	96%	24000	2.38	112.7	238
P(4)(5)	98%	99%	19000	2.07	109.6	256
P(5)(5)	98%	98%	25000	3.33	99.8	259
P(6)(5)	99%	99%	21000	1.55	96.4	307

a. Calculated by ^{1}H NMR ($CDCl_3$, 400 MHz).

b. Measured by GPC using DMF as the eluent (1 mL/min).

c. Measured by DSC at a scanning rate of 10ºC/min.

d. Temperature at weight-loss ratio of 5%, measured by TGA with a heating rate of 20°C/min.

Table S2. Concentrations of polymers and M1 on PE surface[a]. Related to Figure 2 and Figure 6.

		Atom N% (Expected)[b]	Atom N% (Observed)[a]	Concentration on PE surface %	Deviation (%)[c]
A1	**B1**	1.03	1.12	35.88	7.65
	B2	1.10	1.32	39.61	18.84
	B3	1.06	0.87	27.08	-18.75
	B4	0.93	1.06	37.61	12.84
	B5	1.00	1.05	34.65	3.96
A2	**B1**	0.99	1.05	35.00	5.01
	B2	1.05	1.27	39.91	19.74
	B3	1.02	0.99	32.03	-3.90
	B4	0.89	1.06	39.30	17.91
	B5	0.96	1.00	34.38	3.15
A3	**B1**	1.06	1.14	35.49	6.48
	B2	1.13	1.21	35.34	6.03
	B3	1.09	1.24	37.54	12.63
	B4	0.95	1.05	36.47	9.42
	B5	1.03	1.01	32.36	-2.91
A4	**B1**	0.91	0.83	30.10	-9.69
	B2	0.96	1.07	36.78	10.35
	B3	0.94	1.10	38.62	15.87
	B4	0.83	0.84	33.40	0.21
	B5	0.89	1.07	39.67	19.02
A5	**B1**	0.91	0.84	30.46	-8.61
	B2	0.97	1.04	35.38	6.15
	B3	0.94	0.97	34.05	2.16
	B4	0.83	0.85	33.80	1.41
	B5	0.89	0.95	35.22	5.67
A6	**B1**	1.08	1.04	31.78	-4.65
	B2	1.16	1.25	35.56	6.69
	B3	1.12	1.13	33.29	-0.12
	B4	0.97	1.10	37.42	12.27
	B5	1.05	1.07	33.63	0.90
M1		0.92	0.82	29.51	-11.46

a. Measured by X-ray photoelectron spectroscopy (XPS).

b. Calculated according to the bulk concentration (33%).

c. (Concentration on PE surface – 33)/33 × 100%.

Table S3. The fluorescence intensity of *E. coli* and *S. aureus* on the sample disks[a]. Related to Figure 2.

		E.coli	**A.E.(%)[b] (*E. coli*)**	***S.aureus***	**A.E.(%)[b] (*S. aureus*)**
PE		3.828±0.653	0	4.386±0.583	0
A1	**B1**	1.528±0.207	60.06	1.034±0.150	76.42
	B2	2.338±0.344	38.92	0.460±0.157	89.51
	B3	2.207±0.281	42.35	2.116±0.271	51.76
	B4	1.042±0.142	72.78	0.004±0.001	99.91
	B5	0.805±0.103	78.97	1.962±0.240	55.27
A2	**B1**	0.790±0.111	79.36	1.703±0.257	61.17
	B2	1.397±0.158	63.51	3.806±0.519	13.22
	B3	0.511±0.086	86.65	1.721±0.251	60.78
	B4	0.244±0.036	93.63	0.816±0.114	80.37
	B5	1.211±0.172	68.36	1.827±0.238	58.34
A3	**B1**	0.248±0.039	93.52	1.896±0.250	56.77
	B2	1.076±0.120	71.89	2.283±0.307	47.95
	B3	1.032±0.130	73.04	2.112±0.271	51.85
	B4	0.532±0.071	86.10	2.968±0.392	32.33
	B5	2.276±0.316	40.54	1.421±0.186	67.60
A4	**B1**	0.004±0.001	99.90	0.004±0.001	99.91
	B2	0.244±0.036	93.63	0.816±0.114	80.37
	B3	0.097±0.019	97.47	0.237±0.032	95.60
	B4	0.002±0.000	99.95	0.004±0.001	99.91
	B5	1.164±0.162	69.59	0.053±0.010	98.79
A5	**B1**	0.786±0.119	79.47	1.311±0.178	70.11
	B2	1.818±0.237	52.51	1.601±0.227	63.50
	B3	1.456±0.207	61.96	2.407±0.312	45.12
	B4	0.142±0.024	96.29	0.427±0.041	90.26
	B5	0.130±0.013	96.60	2.396±0.307	45.37
A6	**B1**	1.157±0.158	69.78	1.182±0.157	73.12
	B2	0.664±0.097	82.65	2.968±0.407	32.33
	B3	0.708±0.109	81.50	2.431±0.327	44.57
	B4	0.711±0.103	81.43	2.270±0.307	48.24
	B5	1.728±0.206	54.86	2.622±0.339	40.22

a. 37°C, 72 h culture.

b. The antibacterial efficiency (A.E.) of polymers, PE served as the control.

Table S4. The fluorescence intensity of the bacterial on sample disks[a]. Related to Figure 3.

		%[b]	*E.coli*	A.E.(%)[c] (*E. coli*)	*S.aureus*	A.E.(%)[c] (*S. aureus*)
P(4)(1)	PE	33	0.004±0.001	99.90	0.004±0.001	99.91
		20	0.304±0.029	92.06	0.693±0.101	84.20
		10	2.323±0.347	39.32	0.650±0.089	85.18
		5	2.130±0.309	44.36	1.418±0.517	67.67
		0	3.828±0.653	0	4.386±0.583	0
	PP	33	0.010±0.001	99.75	0.003±0.001	99.90
		20	0.340±0.059	91.52	0.406±0.051	86.97
		10	1.417±0.199	64.65	1.256±0.189	59.69
		5	1.555±0.187	61.20	2.080±0.331	33.25
		0	4.008±0.527	0.00	3.116±0.402	0
	PET	33	0.008±0.001	99.77	0.007±0.001	99.78
		20	0.599±0.087	82.73	0.232±0.039	92.70
		10	0.780±0.116	77.52	0.662±0.102	79.16
		5	2.080±0.287	40.04	1.962±0.379	38.22
		0	3.469±0.716	0	3.176±0.394	0
	PMMA	33	0.011±0.002	99.72	0.009±0.001	99.72
		20	0.056±0.011	98.59	0.090±0.010	97.18
		10	0.571±0.071	85.66	0.424±0.057	86.71
		5	1.481±0.249	62.82	1.681±0.210	47.30
		0	3.983±0.497	0	3.190±0.422	0
	PA-66	33	0.009±0.001	99.78	0.010±0.002	99.75
		20	0.840±0.146	79.43	0.159±0.029	96.03
		10	1.061±0.267	74.02	0.746±0.175	81.37
		5	1.654±0.257	59.50	1.598±0.264	60.09
		0	4.084±0.622	0	4.004±0.517	0
P(4)(3)	PE	33	0.002±0.001	99.95	0.004±0.001	99.91
		20	0.050±0.008	98.69	0.254±0.048	94.21
		10	0.330±0.069	91.38	0.616±0.089	85.96
		5	1.601±0.248	58.18	2.010±0.421	54.17
		0	3.828±0.653	0	4.386±0.583	0
	PP	33	0.007±0.001	99.83	0.003±0.001	99.90
		20	0.316±0.041	92.12	0.267±0.037	91.43
		10	1.589±0.308	60.35	1.425±0.245	54.27
		5	1.973±0.307	50.77	1.737±0.207	44.26
		0	4.008±0.527	0	3.116±0.402	0
	PET	33	0.015±0.003	99.57	0.007±0.002	99.78
		20	0.221±0.037	93.63	0.242±0.037	92.38
		10	1.112±0.200	67.94	1.110±0.145	65.05
		5	1.549±0.194	55.35	1.447±0.206	54.44
		0	3.469±0.716	0	3.176±0.394	0
	PMMA	33	0.007±0.002	99.82	0.004±0.001	99.87
		20	0.126±0.027	96.84	0.254±0.038	92.04
		10	0.362±0.042	90.91	0.426±0.057	86.65
		5	1.438±0.037	63.90	1.419±0.029	55.52
		0	3.983±0.497	0	3.190±0.422	0
	PA-66	33	0.018±0.004	99.56	0.014±0.003	99.65
		20	0.183±0.028	95.52	0.155±0.028	96.13
		10	1.732±0.207	57.59	0.767±0.107	80.84
		5	1.708±0.216	58.18	1.115±0.270	72.15
		0	4.084±0.622	0	4.004±0.517	0
P(4)(4)	PE	33	0.004±0.001	99.90	0.013±0.005	99.70
		20	0.340±0.049	91.12	0.211±0.049	95.19
		10	0.491±0.097	87.17	0.695±0.109	84.15
		5	0.553±0.105	85.55	1.291±0.208	70.57
		0	3.828±0.653	0	4.386±0.583	0

PP	33	0.018±0.004	99.55	0.028±0.009	99.10
	20	0.157±0.022	96.08	0.216±0.047	93.07
	10	0.244±0.039	93.91	0.308±0.044	90.12
	5	0.829±0.100	79.32	1.122±0.112	63.99
	0	4.008±0.527	0	3.116±0.402	0
PET	33	0.019±0.002	99.45	0.005±0.002	99.84
	20	0.083±0.014	97.61	0.233±0.057	92.66
	10	0.303±0.049	91.27	0.671±0.094	78.87
	5	1.481±0.027	57.31	1.462±0.028	53.97
	0	3.469±0.716	0	3.176±0.394	0
PMMA	33	0.007±0.001	99.82	0.012±0.003	99.62
	20	0.004±0.001	99.90	0.077±0.022	97.59
	10	0.193±0.038	95.15	0.194±0.029	93.92
	5	0.694±0.103	82.58	0.390±0.062	87.77
	0	3.983±0.497	0	3.190±0.422	0
PA-66	33	0.009±0.001	99.78	0.007±0.001	99.83
	20	0.095±0.017	97.67	0.299±0.042	92.53
	10	0.313±0.041	92.34	0.542±0.071	86.46
	5	1.250±0.203	69.39	1.055±0.151	73.65
	0	4.084±0.622	0	4.004±0.517	0

a. 37°C, 72 h culture.

b. The ratio of selected polymers (**P(4)(1,3,4)**) added in several typical commodity polymers.

c. The antibacterial efficiency (A.E.) of polymers. Commodity polymers served as the controls.

Table S5. Interaction between polymers and polysacchorides[a]. Related to Figure 5.

	lipopolysaccharide	**peptidoglycan**
P(4)(4)	0.10×10^{-3}	0.14×10^{-3}
PE	0.20×10^{-3}	0.26×10^{-3}

a. Measured by an Octet assay by using a BLI Automated Biosensor.

Transparent Methods

EXPERIMENTAL SECTION

1. Materials

All chemicals and solvents were purchased from commercial sources and used without further purification. 2-(Acetoacetoxy)ethyl methacrylate (AEMA, Aladdin, 95%), cinnamic aldehyde (MREDA, 99%), citronellal (MERYER, 99%), hyacinthin (J&K, 97.5%), myrac aldehyde (Energy, 97%), cyclamen aldehyde (MAKLIN, 92%), phellandral (MAKLIN, 97%), 5,5-dimethyl-1,3-cyclohexanedione (MAKLIN, 99%), 1,3-cyclohexanedione (Shaoyuan, 97%), 5-methyl-1,3-cyclohexanedione (NineDing, 98%), 5-phenyl-1,3-cyclohexanedione (Energy, 97%), 5-n-propyl-1,3-cyclohexanedione (Energy, 97%), ammonium acetate (MAKLIN, 98%), glycine (Ouhe, 98%), 2,2'-azobisisoheptonitrile (ABVN, Energy, 98%), polyethylene (PE, 500 mesh, ZhongLian Plastic), polypropylene (PP, 500 mesh, ZhongLian Plastic), polyethylene terephthalate (PET, 500 mesh, ZhongLian Plastic), poly(methyl methacrylate) (PMMA, 500 mesh, ZhongLian Plastic), polyamide 66 (PA66, 500 mesh, ZhongLian Plastic), poly(ethylene imine) (PEI, M_w ~ 10000, 50 wt/% H_2O), 3-bromo-1-propanol (Ark-Pharm, 97%), methacryloylchloride (HEOWNS, 99%), sodium borohydride ($NaBH_4$, LanGe, 98%). Drinking natural mineral water (Nongfu Spring), orange juice (NFC), drinking pure milk (Jizhi), red wine (ChangYu), coffee (Nestle), black tea (Oriental leaves).

Escherichia coli (*E. coli*), BL21 (competent cell of *E. coli*, Merck Millipore)), Staphylococcus aureus strain (*S. aureus,* CMCC), pCMV-N-mCherry (Beyotime), Luria-Bertani (LB) broth (Gibco), LB agar (Gibco), tryptic soy broth (TSB, Gibco), tryptic soy agar (TSA, Gibco), kanamycin sulfate (inalco), isopropyl β-D-thiogalactoside (IPTG, inalco), phosphatic buffer solution (PBS, Gibco) were used as purchased.

2. Instruments

Gel permeation chromatography (GPC) analyses of polymers were performed using *N, N*-dimethyl formamide (DMF) containing 50 mM LiBr as the eluent. The GPC system is a Shimadzu LC-20AD pump system consisting of an auto injector, a MZ-Gel SDplus 10.0 μm guard column (50 × 8.0 mm, 10^2 Å) followed by two PLgel 5 μm MIXED-D columns (300 × 7.5 mm), and a Shimadzu RID-10A refractive index detector. The system was calibrated with narrow molecular weight distribution polystyrene standards ranging from 200 to 10^6 g mol^{-1}.

NMR spectra were obtained using a JEOL JNM-ECA400 spectrometer for all samples. The ESI-MS data were collected using a Micro TOF-QII Bruker. The FT-IR spectra were recorded in a transmission mode on a Perkin-Elmer Spectrum 100 spectrometer (Waltham, MA, USA).

Differential scanning calorimetry (DSC) was performed using a TA instrument Q2000 operated at a scanning rate of 10°C/min. Thermal gravimetric analysis (TGA) was conducted on a TA instrument Q50 with a heating rate of 20°C/min. The fluorescent

images of bacteria were recorded by a Laser scanning Confocal Microscopy (Zeiss LSM 780). Bio-Rad Electroporator was used for the electrotransformation of *E. coli* and *S. aureus*. The tensile shear strength was measured using an MTS SYSTEMS (CHINA) Co. Ltd. SANS CMT6503 electromechanically universal testing machine. Injection molding was performed by a by micro injection molding machine (WZS10D, Shanghai Xinshuo precision instrument co., LTD). X-ray photoelectron spectroscopy (XPS) data were obtained by an ESCALAB 250 Xi electron spectrometer from VG Scientific using 300 W Al Kα radiation with a pass energy of 100.0 eV; binding energy of all the elements was calibrated relative to the carbon impurity with a C1s at 284.8 eV. Biosensor experiment was performed by BLI (BioLayer Interferometry) on Octet RED96 (Pall ForteBIO LLC, Fremont, USA).

3. Methods

3.1 2-(Methacryloyloxy)ethyl (E)-2,7,7-trimethyl-5-oxo-4-styryl-1,4,5,6,7,8-hexahydroquinoline-3-carboxylate (M(1)(1))

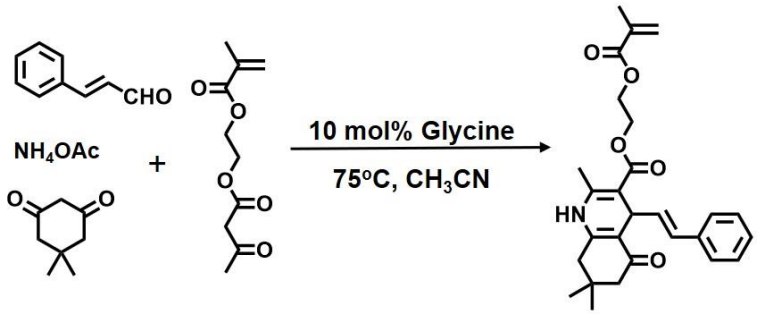

The monomers M(X)(1) were prepared via the Hantzsch reaction by different combinations of aldehydes (A(X)) and 5,5-dimethyl-1,3-cyclohexanedione (B(1)). Typically, A(1) (cinnamaldehyde, 660 mg, 5.0 mmol), AEMA (1.07 g, 5.0 mmol), B(1)

(700 mg, 5.0 mmol), and ammonium acetate (578 mg, 7.5 mmol) were put in a 15-mL centrifuge tube. Then, glycine (38 mg, 0.5 mmol) and acetonitrile (6.0 mL) were added. The mixture was kept in an oil bath (75ºC) for 4 h. After removing volatiles under vacuum, the crude was purified by a column chromatography (petroleum ether/ethyl acetate: 5/1) to get monomer M(1)(1) as a yellow powder (1.65 g, yield: 73.6%).

All other monomers were prepared through the same procedure.

^{1}H NMR (400 MHz, $CDCl_3$, δ/ppm): 7.06-7.29 (m, 5H, ph), 6.20 (s, 1H, CHC<u>H</u>=CH), 6.19 (s, 1H, CHCH=C<u>H</u>), 6.12 (s, 1H, CH_2=C), 6.06 (s, 1H, NH), 5.57 (s, 1H, CH_2=C), 4.54 (s, 1H, CCHC,), 4.25-4.44 (m, 4H, $COOCH_2CH_2$), 2.36 (s, 2H, CH_2C=O), 2.09 (s, 3H, NHCC<u>H</u>$_3$), 2.00 (s, 3H, C<u>H</u>$_3$C=CH_2), 1.90 (s, 2H, NHCC<u>H</u>$_2$), 1.08 (s, 6H, CH_3CCH_3).

^{13}C NMR (100 MHz, $CDCl_3$, δ/ppm): 196.15, 167.70, 167.29, 149.84, 147.27, 145.23, 135.96, 128.02, 127.98, 127.97, 127.96, 127.95, 126.96, 126.95, 126.19, 111.79, 105.18, 62.80, 61.51, 50.93, 40.58, 36.70, 32.70, 29.59, 27.13, 19.29, 18.38.

IR (ν/cm^{-1}): 3287, 2959, 1716, 1692, 1603, 1488, 1377, 1279, 1214, 1149, 1113, 1082, 1045, 941, 884, 814, 783, 695, 658, 566.

ESI-MS: observed (expected): 450.2286 (450.2280) [M + H^+].

3.2 2-(Methacryloyloxy)ethyl 4-(2,6-dimethylhept-5-en-1-yl)-2,7,7-trimethyl-5-oxo-1,4,5,6,7,8-hexahydroquinoline-3-carboxylate (M(2)(1))

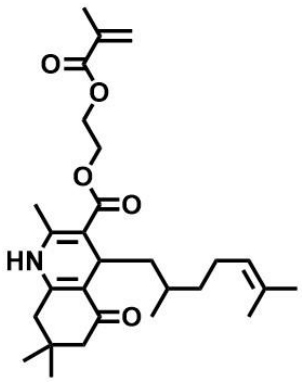

^{1}H NMR (400 MHz, $CDCl_3$, δ/ppm): 6.12 (s, 1H, CH_2=C), 5.83 (s, 1H, NH), 5.57 (s, 1H, CH_2=C), 5.05 (m, 1H, C<u>H</u>=C(CH_3)$_2$), 4.25-4.44 (m, 4H, COOCH_2CH_2), 4.05 (s, 1H, CCHC), 2.36 (s, 2H, CH_2C=O), 2.09 (s, 3H, NHCC<u>H</u>$_3$), 2.00 (s, 3H, C<u>H</u>$_3$C=CH_2), 1.90 (s, 2H, NHCC<u>H</u>$_2$), 1.60 (s, 3H, CH=CC<u>H</u>$_3$), 1.55 (s, 3H, CH=CC<u>H</u>$_3$), 1.25 (m, 7H, C<u>H</u>$_2$C<u>H</u>CH_3C<u>H</u>$_2$C<u>H</u>$_2$), 1.08 (s, 6H, CH_2C(C<u>H</u>$_3$)$_2$), 0.86 (d, 3H, CHC<u>H</u>$_3$, J = 4.2 Hz).

^{13}C NMR (100 MHz, $CDCl_3$, δ/ppm): 196.28, 167.70, 167.27, 148.98, 145.00, 136.03, 130.73, 128.93, 126.21, 112.53, 105.74, 62.85, 61.53, 50.98, 44.86, 41.34, 38.32, 37.49, 32.42, 29.85, 27.70, 27.43, 25.81, 25.62, 20.24, 19.51, 18.40, 17.68.

IR (ν/cm^{-1}): 3675, 3285, 2971, 2901, 1719, 1694, 1637, 1604, 1480, 1451, 1405, 1393, 1319, 1241, 1214, 1164, 1075, 1056, 938, 891, 813, 776, 661.

ESI-MS: observed (expected): 472.3061 (472.3063) [M + H^+].

3.3 2-(Methacryloyloxy)ethyl 4-benzyl-2,7,7-trimethyl-5-oxo-1,4,5,6,7,8-hexahydroquinoline-3-carboxylate (M(3)(1))

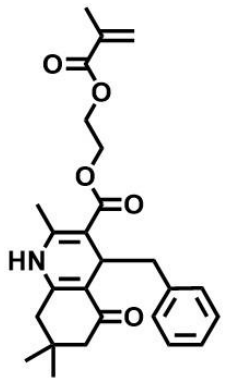

^{1}H NMR (400 MHz, $CDCl_3$, δ/ppm): 6.95-7.25 (m, 5H, ph), 6.12 (s, 1H, CH_2=C), 5.76 (s, 1H, NH), 5.57 (s, 1H, CH_2=C), 4.31 (s, 1H, CCHC), 4.18-4.30 (m, 4H, $COOCH_2CH_2$), 2.62 (m, 2H, $phCH_2$), 2.36 (s, 2H, CH_2C=O), 2.09 (s, 3H, NHCC$\underline{H}_3$), 2.00 (s, 3H, C$\underline{H}_3$C=CH_2), 1.90 (s, 2H, NHCC$\underline{H}_2$), 1.08 (s, 6H, CH_3CCH_3).

^{13}C NMR (100 MHz, $CDCl_3$, δ/ppm): 196.08, 167.99, 167.21, 149.74, 145.27, 137.36, 135.94, 131.24, 126.10, 124.50, 120.43, 110.02, 103.37, 62.74, 61.74, 50.94, 41.99, 41.31, 37.53, 34.11, 32.39, 29.85, 27.63, 26.48, 19.45, 17.67.

IR (ν/cm^{-1}): 3675, 3286, 3062, 2959, 1719, 1693, 1603, 1486, 1452, 1383, 1320, 1296, 1279, 1220, 1165, 1106, 1079, 1048, 1004, 941, 814, 753, 699, 595.

ESI-MS: observed (expected): 438.2287 (438.2280) [M + H^+].

3.4 2-(Methacryloyloxy)ethyl 2,7,7-trimethyl-4-(4-(4-methylpent-3-en-1-yl) cyclohex-3-en-1-yl)-5-oxo-1,4,5,6,7,8-hexahydroquinoline-3-carboxylate (M(4)(1))

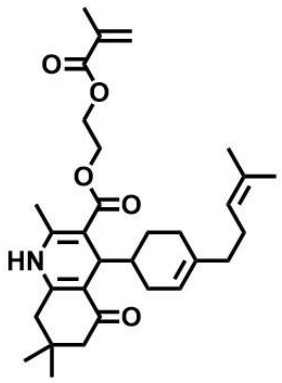

^{1}H NMR (400 MHz, $CDCl_3$, δ/ppm): 6.12 (s, 1H, CH_2=C), 5.95 (s, 1H, NH), 5.57 (s, 1H, CH_2=C), 5.29 (m, 1H, $CHCH_2C\underline{H}$=C), 5.05 (d, 1H, $CH_2CH_2C\underline{H}$=C, J = 6.9 Hz), 4.25-4.44 (m, 4H, $COOCH_2CH_2$), 4.12 (s, 1H, CCHC), 2.36 (s, 2H, $C\underline{H}_2C$=O), 2.09 (s, 3H, $NHCC\underline{H}_3$), 2.00 (s, 3H, $C\underline{H}_3C$=CH_2), 1.95-2.06 (m, 4H, $CC\underline{H}_2C\underline{H}_2CH$), 1.70-2.10 (m, 7H, $CH_2CHCH_2CH_2$), 1.90 (s, 2H, $NHCC\underline{H}_2$), 1.81 (s, 3H, $CHCC\underline{H}_3$), 1.76 (s, 3H, $CHCC\underline{H}_3$), 1.08 (s, 6H, CH_3CCH_3).

^{13}C NMR (100 MHz, $CDCl_3$, δ/ppm): 196.08, 167.80, 167.21, 149.70, 145.27, 137.36, 135.97, 131.24, 126.10, 124.50, 120.43, 110.14, 103.37, 62.74, 61.47, 50.97, 41.99, 41.31, 37.53, 34.11, 32.39, 29.85, 29.23, 27.63, 27.34, 26.48, 25.70, 19.48, 18.30, 18.30, 17.67.

IR (ν/cm^{-1}): 3675, 3281, 2968, 2901, 1720, 1694, 1606, 1483, 1383, 1280, 1214, 1153, 1105, 1076, 1045, 997, 938, 883, 788, 754, 610, 588, 565.

ESI-MS: observed (expected): 510.3224 (510.3219) [M + H^+].

3.5 2-(Methacryloyloxy)ethyl 4-(1-(4-isopropylphenyl)propan-2-yl)-2,7,7-trimethyl-5-oxo-1,4,5,6,7,8-hexahydroquinoline-3-carboxylate (M(5)(1))

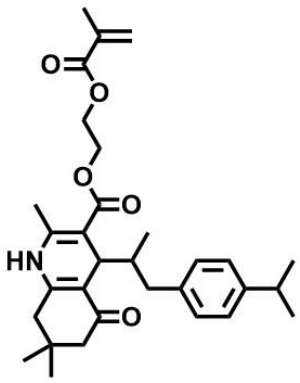

^{1}H NMR (400 MHz, $CDCl_3$, δ/ppm): 6.95-7.09 (m, 4H, ph), 6.12 (s, 1H, CH_2=C), 5.89 (s, 1H, NH), 5.57 (s, 1H, CH_2=C), 4.32-4.44 (m, 4H, $COOCH_2CH_2$), 4.19 (s, 1H, CCHC), 2.92 (m, 2H, CH_2ph), 2.30 (m, 1H, phCH), 2.36 (s, 2H, CH_2C=O), 2.09 (s, 3H, NHCC$\underline{H}_3$), 2.00 (s, 3H, C$\underline{H}_3$C=CH_2), 1.90 (s, 2H, NHCC$\underline{H}_2$), 1.55-1.65 (m, 1H, $CH_2C\underline{H}CH_3$), 1.10 (d, 3H, $CH_2CHC\underline{H}_3$, J = 6.5 Hz), 1.08 (s, 6H, CH_3CCH_3), 0.67 (d, 6H, C$\underline{H}_3$CHC$\underline{H}_3$, J = 6.5 Hz).

^{13}C NMR (100 MHz, $CDCl_3$, δ/ppm): 197.13, 167.23, 164.74, 146.93, 139.16, 137.36, 135.94, 135.41, 129.02, 126.51, 126.07, 125.03, 124.04, 110.04, 103.57, 63.15, 62.36, 51.98, 46.55, 40.24, 33.78, 32.99, 32.40, 30.03, 28.36, 27.19, 25.31, 24.16, 18.37, 17.87, 15.22.

IR (ν/cm^{-1}): 3285, 2958, 1720, 1697, 1604, 1483, 1382, 1275, 1217, 1150, 1113, 1076, 1048, 998, 938, 886, 856, 812, 783, 654, 590, 566, 554.

ESI-MS: observed (expected): 508.3069 (508.3063) [M + H^+].

3.6 2-(Methacryloyloxy)ethyl 4-hexyl-2,7,7-trimethyl-5-oxo-1,4,5,6,7,8-hexahydroquinoline-3-carboxylate (M(6)(1))

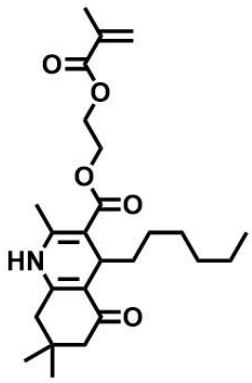

^{1}H NMR (400 MHz, $CDCl_3$, δ/ppm): 6.12 (s, 1H, CH_2=C), 6.05 (s, 1H, NH), 5.57 (s, 1H, CH_2=C), , 4.25-4.44 (m, 4H, $COOCH_2CH_2$), 4.00 (s, 1H, CCHC), 2.36 (s, 2H, CH_2C=O), 2.09 (s, 3H, NHCC$\underline{H}_3$), 2.00 (s, 3H, C$\underline{H}_3$C=CH_2), 1.90 (s, 2H, NHCC$\underline{H}_2$), 1.09-1.50 (m, 10H, CH(C$\underline{H}_2$)$_5$$CH_3$), 1.08 (s, 6H, CH_3CCH_3), 0.86 (s, 3H, CH_2C$\underline{H}_3$).

^{13}C NMR (100 MHz, $CDCl_3$, δ/ppm): 196.14, 167.62, 167.29, 149.90, 145.38, 136.08, 126.15, 111.33, 104.67, 62.81, 61.47, 51.02, 41.08, 36.34, 32.59, 32.01, 29.84, 29.75, 27.09, 25.01, 22.76, 19.43, 18.36, 14.16, 14.15.

IR (ν/cm^{-1}): 3281, 2926, 1722, 1693, 1605, 1483, 1386, 1278, 1216, 1163, 1094, 1048, 995, 954, 884, 813, 780, 747, 641, 618, 587, 575, 558.

ESI-MS: observed (expected): 432.2759 (432.2750) [M + H^+].

3.7 Polymerization of M(X)(1) to get P(X)(1)

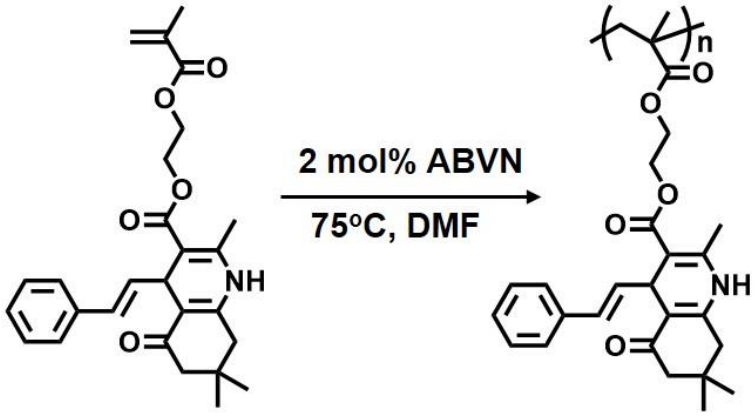

The ‘pure’ polymers P(X)(1) were prepared by radical polymerization of M(X)(1). For example, monomer M(1)(1) (450 mg, 1.0 mmol), 2,2'-azobis-(2,4-dimethylvaleronitrile) (ABVN, 5 mg, 0.02 mmol) were dissolved in dimethyl formamide (DMF, 1.0 mL). The mixture was purged by nitrogen flow for 20 min, then kept in an oil bath (75°C) for 12 h. The polymerization was quenched in an ice−water bath. After precipitation in diethyl ether three times, P(1)(1) was obtained as a yellow powder (400 mg, yield: 88.9%).

All other ‘pure’ polymers were prepared through the same procedure by using different monomers.

3.8 HTP-One pot preparation of polymers (P(X)(Y))

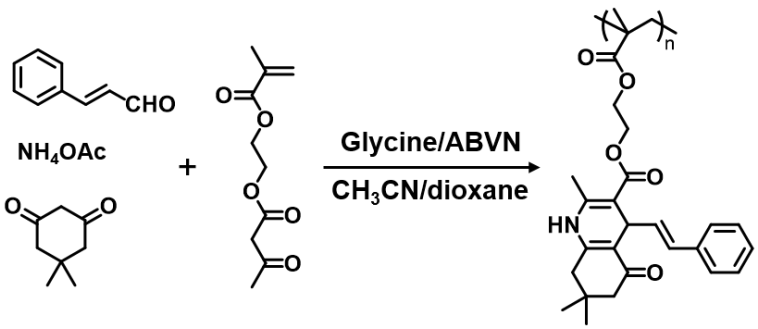

Polymers P(X)(Y) were prepared *via* a one-pot HTP method. For a representative synthesis, A(1) (cinnamaldehyde, 660 mg, 5.0 mmol), AEMA (1.07 g, 5.0 mmol), B(1) (5,5-dimethyl-1,3-cyclohexanedione, 700 mg, 5.0 mmol), and ammonium acetate (578 mg, 7.5 mmol) were charged to a 15-mL centrifuge tube. Then, glycine (38 mg, 0.5 mmol), ABVN (25 mg, 0.1 mmol), and acetonitrile/1,4-dioxane (3.0/3.0 mL) were added. The mixture was purged by bubbling nitrogen for 20 min, then sealed and placed in an oil bath (75°C) for 12 h. The polymerization was quenched in an ice–water bath. A 20–50 μL aliquot was taken for ^{1}H NMR and GPC analyses. The polymer was purified by precipitation in water followed by re-precipitation from THF with diethyl ether to obtain a yellow powder (P(1)(1) (1.85 g, yield: 82.3%).

All other polymers were simultaneously prepared using the same procedure with the respective A and B starting materials.

3.9 Red-fluorescent-protein (RFP) transferred bacteria

RFP transferred bacteria were prepared according to previous literatures(Nickoloff, 1995). BL21 is a competent cell line of *E. coli*. BL21 cells were transferred to a chilled electroporation cuvette with a precooled plasmid solution (2 μL, pCMV-N-mCherry in PBS, 100 μg/mL, kanamycin resistance). This cuvette was put in the electroporation instrument for electric shock with an exponential decay pulse (2.5 kV, 200-Ω resistance, 25-μF capacitance, 4.5 ms). Then, LB medium (1 mL) was added to the electroporation cuvette, and the contents were transferred to a 1.5-mL tube for incubation (1.5 h, 180 r/min, 37°C). The mixture was plated on a LB agar plate containing antibiotic

(kanamycin sulfate: 50 μg/mL) and incubated at 37°C for 12 h. One small colony was isolated and incubated in 200 mL of LB medium for 2 h. Then, IPTG (200 mM, 2 mL) was added to induce gene expression (28°C, 4 h) to obtain the RFP-*E. coli*.

RFP-*S. aureus* was similarly prepared.

3.10 Poly(acetoacetoxy ethyl methacrylate) (P(AEMA))

AEMA (2.14 g, 10 mmol) and ABVN (50 mg, 0.2 mmol) were dissolved in DMF (20 mL) and put in a 50 mL polymerization tube. This tube was sealed with a rubber septum and purged by nitrogen flow for 20 min, and kept in an oil bath (75^{o}C) for 12 h. The polymerization was quenched in an ice−water bath, and the polymer (P(AEMA)) was purified by precipitation in diethyl ether three times as a white powder (1.82 g, yield: 85.0%).

3.11 Poly((4-(4-methylpent-3-en-1-yl)cyclohex-3-en-1-yl)methyl methacrylate) (P1)

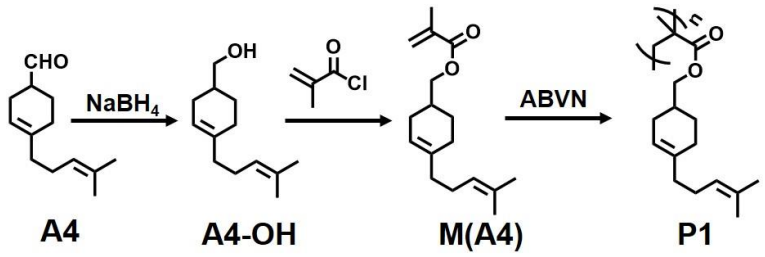

A4-OH: Myrac aldehyde (A4, 9.62 g, 50 mmol) and sodium borohydride ($NaBH_4$, 2.27 g, 60 mmol) were dissolved in methanol (50 mL), and put in an ice bath for 4 h. After removing volatiles under vacuum, A4-OH was purified by a column chromatography (petroleum ether/ethyl acetate = 10/1) as a colorless oil (8.59 g, 88.4% yield).

^{1}H NMR (400 MHz, $CDCl_3$, δ/ppm): 5.45 (d, 1H, $CHCH_2C\underline{H}$=C, *J* = 6.8 Hz), 5.05 (t, 1H, $CH_2CH_2C\underline{H}$=C, *J* = 6.9 Hz), 3.58 (m, 2H, $C\underline{H}_2OH$), 2.20-2.10 (m, 7H, $CH_2CHCH_2CH_2$), 2.10-2.00 (m, 4H, $C\underline{H}_2C\underline{H}_2CH$=$C(CH_3)_2$), 1.85 (s, 3H, CH=$CC\underline{H}_3CH_3$), 1.82 (s, 3H, CH=$CCH_3C\underline{H}_3$).

^{13}C NMR (100 MHz, $CDCl_3$, δ/ppm): 137.89, 131.47, 124.44, 119.54, 67.91, 37.79, 36.44, 28.30, 27.88, 26.55, 25.79, 25.75, 17.77.

IR (ν/cm^{-1}): 3324, 2965, 2913, 1670, 1437, 1376, 1261, 1232, 1139, 1087, 1049, 943, 892, 825, 673, 600, 581, 563.

ESI-MS: observed (expected): 195.1757 (195.1749) [M + H^+].

M(A4): A4-OH (1.94 g, 10 mmol) and trimethylamine (2.0 g, 20 mmol) was solved in CH_2Cl_2 (20 mL) followed by adding methacryloyl chloride (1.3 g, 12 mmol) dropwise slowly. The mixture was kept at 20°C for 6 h. M(A4) was purified by a column chromatography (petroleum ether/ethyl acetate = 10/1) as a colorless oil (1.95 g, 74.4% yield).

^{1}H NMR (400 MHz, $CDCl_3$, δ/ppm): 6.12 (s, 1H, $C\underline{H}_2$=CCH_3), 5.67 (s, 1H, $C\underline{H}_2$=CCH_3), 5.45 (d, 1H, $CHCH_2C\underline{H}$=C, *J* = 6.8 Hz), 5.05 (d, 1H, $CH_2CH_2C\underline{H}$=C, *J* = 6.9 Hz), 3.58 (m, 2H, $CHC\underline{H}_2O$), 2.10-2.20 (m, 7H, $CH_2CHCH_2CH_2$), 2.00-2.10 (m, 4H, $C\underline{H}_2C\underline{H}_2CH$=C), 2.00 (s, 3H, $C\underline{H}_3C$=CH_2),1.85 (s, 3H, CH=$CC\underline{H}_3CH_3$), 1.82 (s, 3H, CH=$CCH_3C\underline{H}_3$).

^{13}C NMR (100 MHz, $CDCl_3$, δ/ppm): 167.63, 137.82, 136.62, 131.52, 125.32, 124.38, 119.25, 69.01, 37.76, 33.21, 28.45, 27.73, 26.53, 25.87, 25.79, 18.44, 17.77.

IR (ν/cm^{-1}): 3676, 2967, 2914, 1718, 1638, 1452, 1403, 1376, 1320, 1296, 1104, 1066, 1049, 1013, 984, 937, 813, 760, 726, 683, 580.

ESI-MS: observed (expected): 285.1839 (285.1831) [M + Na^{+}].

P1: M(A4) (2.62 g, 10 mmol) and ABVN (50 mg, 0.1 mmol) were dissolved in DMF (20 mL). The mixture was purged by nitrogen flow for 20 min, and kept in an oil both (75ºC) for 12 h. The polymerization was quenched in an ice−water bath, and P1 was precipitated in diethyl ether three times as a white powder (2.08 g, 79.4% yield).

3.12 Poly(3-(2,6-dioxo-4-phenylcyclohexyl)propyl methacrylate) (P2)

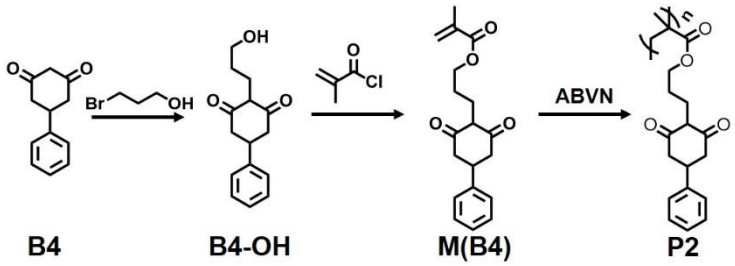

B4-OH: 5-Phenyl-1,3-cyclohexanedione (B4, 9.40 g, 50 mmol), potassium iodide (KI, 10 g, 60 mmol), potassium carbonate (K_2CO_3, 13.8 g, 50 mmol) and 3-bromo-1-propanol (6.9 g, 50 mmol) were dissolved in acetone (50 mL). This solution was refluxed for 12 h. After removing acetone under vacuum, B4-OH was purified by a column chromatography (petroleum ether/ethyl acetate = 5/1) as a colorless oil (8.86 g, 72.1% yield).

^{1}H NMR (400 MHz, $CDCl_3$, δ/ppm): 7.10-7.45 (m, 5H, ph), 5.48 (s, 1H, $CH_2O\underline{H}$), 4.06 (m, 2H, $C\underline{H}_2OH$), 3.92 (m, 1H, CCHC), 3.41 (t, 1H, $CH_2C\underline{H}CH_2$, J = 5.2 Hz), 2.62 (m, 4H, $C\underline{H}_2CHC\underline{H}_2$), 2.60 (m, 2H, $CHC\underline{H}_2CH_2$), 2.00 (m, 2H, $C\underline{H}_2CH_2OH$).

^{13}C NMR (100 MHz, $CDCl_3$, δ/ppm): 199.18, 199.18, 142.70, 128.90, 128.90, 127.17, 126.77, 126.77, 67.75, 62.27, 43.91, 43.91, 39.43, 36.71, 31.50.

IR (ν/cm^{-1}): 3403, 3029, 2944, 1717, 1598, 1497,1465,1453,1399,1374,1352, 1265, 1231, 1209, 1139, 1089,1061, 1000, 968, 868, 825, 760, 733, 699, 657, 615, 600.

ESI-MS: observed (expected): 247.1339 (247.1334) [M + H^+].

M(B4): B4-OH (2.5 g, 10 mmol) and trimethylamine (2.0 g, 20 mmol) were solved in CH_2Cl_2 (25 mL). Methacryloyl chloride (1.3 g, 12 mmol) was added dropwise slowly. The mixture was kept at 25ºC for 1 h. After removing the white solid by filtration and the volatiles under vacuum, M(B4) was purified by a column chromatography (petroleum ether/ethyl acetate = 5/1) as a colorless oil (2.67 g, 85.1% yield).

^{1}H NMR (400 MHz, $CDCl_3$, δ/ppm): 7.10-7.45 (m, 5H, ph), 6.12 (s, 1H, CH_2=C), 5.57 (s, 1H, CH_2=C), 4.21 (t, 2H, C$\underline{H_2}$O, *J* = 6.2 Hz), 4.02 (m, 1H, CCHC), 3.41 (t, 1H, $CH_2C\underline{H}CH_2$, *J* = 6.7 Hz), 2.62 (m, 4H, C$\underline{H_2}$CHC$\underline{H_2}$), 2.60 (m, 2H, CHC$\underline{H_2}CH_2$), 2.00 (m, 2H, $CH_2C\underline{H_2}CH_2$), 1.98 (s, 3H, CH_2=C$C\underline{H_3}$).

^{13}C NMR (100 MHz, $CDCl_3$, δ/ppm): 198.93, 176.91, 167.34, 142.68, 136.19, 128.90, 128.90, 127.16, 126.77, 126.77, 125.91, 102.80, 65.38, 61.08, 43.91, 39.40, 36.60, 28.06, 18.40.

IR (ν/cm^{-1}): 3675, 2958, 2901, 1716, 1654, 1602, 1497, 1469, 1454, 1428, 1403, 1374, 1351, 1318, 1296, 1257, 1231, 1207, 1161, 1044, 1007, 975, 940, 910, 869, 816, 760, 733, 699, 656, 613, 588.

ESI-MS: observed (expected): 337.1422 (337.1416) [M + Na^+].

P2: M(B4) (1.57 g, 10 mmol) and ABVN (50 mg, 0.2 mmol) were dissolved in DMF (20 mL). This solution was purged by nitrogen flow for 20 min, then kept in an oil bath (75°C) for 12 h. The polymerization was quenched in an ice−water bath. P2 was purified by precipitation in diethyl ether three times as a white powder (1.37 g, 87.3% yield).

3.13 Ethyl 2-methyl-4-(4-(4-methylpent-3-en-1-yl)cyclohex-3-en-1-yl)-5-oxo-7-phenyl-1,4,5,6,7,8-hexahydroquinoline-3-carboxylate (M1)

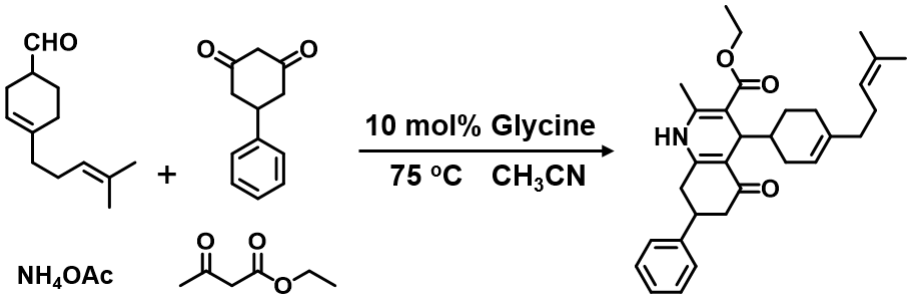

Myrac aldehyde (A(4), 1.92 g, 10 mmol), ethyl acetoacetate (1.30 g, 10 mmol), 5-phenyl-1,3-cyclohexanedione (B(4), 1.89 g, 10 mmol), and ammonium acetate (1.16 g, 15 mmol) were put in a 15-mL centrifuge tube. Then, glycine (76 mg, 1 mmol) and acetonitrile (9.0 mL) were added. The mixture was kept in an oil bath (75°C) for 4 h. Acetonitrile was removed under vacuum, and the crude was purified by a column chromatography (petroleum ether/ethyl acetate: 5/1) to get M1 as a yellow oil (3.86 g, yield: 81.6%).

^{1}H NMR (400 MHz, $CDCl_3$, δ/ppm): 7.10-7.33 (m, 5H, ph), 6.08 (s, 1H, NH), 5.29 (s, 1H, $CHCH_2C\underline{H}$=C), 5.09 (s, 1H, $CH_2CH_2C\underline{H}$=C), 4.13 (m, 2H, $C\underline{H}_2O$), 4.12 (s, 1H,

CCHC), 3.51 (m, 1H, phC<u>H</u>), 2.36 (m, 2H, CH_2C=O), 2.09 (s, 3H, NHCC<u>H_3</u>), 1.90 (s, 2H, NHCC<u>H_2</u>), 1.95-2.06 (m, 4H, CC<u>H_2</u>C<u>H_2</u>CH), 1.70-2.10 (m, 7H, $CH_2CHCH_2CH_2$), 1.81 (s, 3H, CHCC<u>H_3</u>), 1.76 (s, 3H, CHCC<u>H_3</u>), 1.17 (m, 3H, C<u>H_3</u>CH_2O).

^{13}C NMR (100 MHz, $CDCl_3$, δ/ppm): 195.62, 168.44, 150.57, 144.00, 142.64, 137.34, 131.33, 128.79, 128.79, 127.05, 126.84, 126.84, 124.61, 120.49, 111.40, 104.00, 59.88, 43.78, 41.97, 41.57, 39.58, 37.64, 34.90, 34.55, 29.32, 27.68, 26.63, 25.80, 19.36, 17.78, 14.49.

IR (ν/cm^{-1}): 3288, 2980, 2908, 1738, 1696, 1641, 1605, 1485, 1449, 1372, 1236, 1215, 1157, 1105, 1070, 1045, 937, 915, 846, 786, 762, 699, 634, 607, 560.

ESI-MS: observed (expected): 474.3015 (474.3008) [M + H^+].

3.14 HTP measurements of the antibacterial ability of polymers

Preliminary screening: As a typically example, P(1)(1) (1.5 g) and PE powder (3.0 g) were mixed and grinded evenly in a mortar. The mixture was manufactured to a square membrane (40 × 40 mm, thickness: 0.5 mm) by the hot-press technology under 150°C. Then, P(1)(1)-PE discs (diameter: 5 mm) were prepared by using a puncher. Other P(X)(Y)-PE samples were similarly prepared.

All P(X)(Y)-PE samples were attached on glass slides (25 mm × 75 mm × 1 mm) to get mini-arrays (10 samples/piece). These mini-arrays were used to test the antibacterial ability of P(X)(Y) with PE as the control. Briefly, these polymer mini-arrays were sterilized by a 75% ethanol aqueous solution and UV light (254 nm, 40 w, 30 min), then put into a Luria-Bertani (LB) broth (200 mL) followed by addition of a

suspension of planktonic *E. coli* or *S. aureus* (10 μL). The optical density of this suspension at UV~600 nm (OD600) is approximately 1.0. The polymer arrays were incubated with bacteria for 72 h followed by washing twice with water and fixation with paraformaldehyde (4%) prior to observation by laser scanning confocal microscopy (LSCM, excitation wavelength: 543 nm; emission wavelength: 566–719 nm).

Secondary screening: P(X)(Y)-polymer samples were prepared by abovementioned method. These samples were attached on glass slides for antibacterial test as abovementioned. Commodity polymers (PE, PP, PET, PMMA, PA-66) were used as the controls.

Antibacterial capabilities of all other polymers and small molecules (PEI, P(AEMA), P1, P2, and M1) were similarly tested through the polymer-array method.

3.15 Mechanical properties of P(4)(4)-polymer samples

The tensile shear strength of P(4)(4)-polymer samples were tested according to the national standard method (GBT 1040.3-2006). As a typical example, P(4)(4) (5 g) was mixed with PE (10 g) to prepare dumbbell-shaped splines by hot pressing. The dumbbell-shaped splines were in agreement with the national standard (length: 120 mm, breadth: 25 mm, thickness: 0.5 mm; length of narrow part: 25 mm, breadth of narrow part: 6 mm, thickness of narrow part: 0.5 mm). These splines were tested by an MTS SYSTEMS (CHINA) Co. Ltd. SANS CMT6503 electromechanically universal testing machine (tensile speed: 5 mm/min; 25°C).

All other P(4)(4)-polymer splines were prepared and tested through the same procedure. General polymers were used as the controls. The data are presented as mean ± SD (n = 6).

3.16 Injection molding for plastic bowls

The plastic bowls were produced by injection molding technology. Typically, the uniform mixture of P(4)(4)-PE (33 wt.% of P(4)(4), 3 g) was added to the machine and heated (150 °C, 2 minutes) to melt-down. Then, the molten polymer was injected into a mold for bowl (0.6 Mpa, 1 minute) followed by keeping at 25°C (normal atmosphere, 10 minutes) to get a plastic P(4)(4)-PE bowl.

The PE bowls were prepared through the same procedure.

3.17 Antibacterial capability of bowls

The antibacterial capability of bowls has been characterized according to a standard method (QB/T2591-2003). Briefly, bowls were sterilized by a 75% ethanol aqueous solution, and incubated with a suspension of *S. aureus* in LB medium (5 mL, OD600 = 1.0) for 24 h at 37ºC. Then, these bowls were washed with sterilized PBS for 10 times prior to addition of different beverages (drinking natural mineral water (Nongfu Spring), orange juice (NFC), drinking pure milk (Jizhi), red wine (ChangYu), coffee (Nestle), black tea (Oriental leaves)) (5 mL). These bowls containing beverages were covered with glass and incubated at 37°C. Aliquots were taken at different time intervals for analyses.

The experiment to simulate actual application of bowls was similarly performed by keeping bowls on a laboratory bench (face up) for 24 h prior to adding different beverages.

3.18 Plate-streaking experiment

A plate-streaking experiment was performed to test for the presence of viable bacteria. Typically, after 24 h culture, beverage aliquots (100 μL) were taken and evenly coated on the surface of LB agar-coated petri dishes (diameter: 90 mm, thickness: 6 mm, LB: 1.5 g/L). These petri dishes were incubated at 37°C for 24 h prior to observation. Original beverages were used as the controls.

Beverage samples taken at 48 h and 72 h were similarly tested.

3.19 Interaction between P(4)(4) and polysaccharides

The interaction between P(4)(4) and two polysaccharides on bacteria surface (lipopolysaccharide and peptidoglycan) were tested via an Octet assay(Abdiche et al., 2008) by using a BLI Automated Biosensor. Streptavidin (SA) biosensors and kinetic buffer (PBS, 0.02% Tween) were used. Each polysaccharide (1 μg/mL) was biotinylated by Sulfo-NHS-Biotin (Pierce Biotechnology, Rockford, IL) at a 1:1 ratio. P(4)(4) was dissolved in DMSO (0.1 mL, 400 μg/mL) then added in the kinetics buffer (1.9 mL) prior to measurement.

3.20 Statistical Analyses

Results were analyzed with SPSS 25.0 and MedCalc 18.1 and are presented as mean ± SD as indicated. Comparisons were performed between two groups using a two-tailed Student's t-test or ANOVA test when comparing more than two conditions. For all analyses, $*p < 0.05$ and $**p < 0.01$ were considered statistically significant. Each experiment was carried out at least three times independently. The sample size is pre-estimated to ensure statistical analysis and no sample was optionally excluded from analysis. No blinding was done in the analyses and quantifications.

Reference:

Abdiche, Y., Malashock, D., Pinkerton, A., and Pons, J. (2008). Determining kinetics and affinities of protein interactions using a parallel real-time label-free biosensor, the Octet. Anal Biochem *377*, 209-217.

Nickoloff, J.A. (1995). Electroporation protocols for microorganisms (Totowa, N.J.: Humana Press).